244

0-315-12555-1

National Library of Canada | Bibliothèque nationale du Canada

Canadian Theses Division | Division des thèses canadiennes

Ottawa, Canada
K1A 0N4

60466

PERMISSION TO MICROFILM — AUTORISATION DE MICROFILMER

• Please print or type — Écrire en lettres moulées ou dactylographier

Full Name of Author — Nom complet de l'auteur

Christie Judith Ryan

Date of Birth — Date de naissance

20/05/55

Country of Birth — Lieu de naissance

Canada

Permanent Address — Résidence fixe

RR # 1 Deep River, Ont
K0J 1P0

Title of Thesis — Titre de la thèse

Orientational Dependence of Surface Energy at the Ice-Water Interface.

University — Université

~~University of ALBERTA~~

Degree for which thesis was presented — Grade pour lequel cette thèse fut présentée

~~M.Sc.~~ University of Alberta

M Sc

Year this degree conferred — Année d'obtention de ce grade

1982

Name of Supervisor — Nom du directeur de thèse

Dr. Tom Forest

Permission is hereby granted to the NATIONAL LIBRARY OF CANADA to microfilm this thesis and to lend or sell copies of the film.

The author reserves other publication rights, and neither the thesis nor extensive extracts from it may be printed or otherwise reproduced without the author's written permission.

L'autorisation est, par la présente, accordée à la BIBLIOTHÈQUE NATIONALE DU CANADA de microfilmer cette thèse et de prêter ou de vendre des exemplaires du film.

L'auteur se réserve les autres droits de publication; ni la thèse ni de longs extraits de celle-ci ne doivent être imprimés ou autrement reproduits sans l'autorisation écrite de l'auteur.

Date

July 13/82

Signature

Christie Ryan

NL-91 (4/77)

CANADIAN THESES ON MICROFICHE

I.S.B.N.

THESES CANADIENNES SUR MICROFICHE

National Library of Canada
Collections Development Branch

Canadian Theses on
Microfiche Service

Ottawa, Canada
K1A 0N4

Bibliothèque nationale du Canada
Direction du développement des collections

Service des thèses canadiennes
sur microfiche

NOTICE

The quality of this microfiche is heavily dependent upon the quality of the original thesis submitted for microfilming. Every effort has been made to ensure the highest quality of reproduction possible.

If pages are missing, contact the university which granted the degree.

Some pages may have indistinct print especially if the original pages were typed with a poor typewriter ribbon or if the university sent us a poor photocopy.

Previously copyrighted materials (journal articles, published tests, etc.) are not filmed.

Reproduction in full or in part of this film is governed by the Canadian Copyright Act, R.S.C. 1970, c. C-30. Please read the authorization forms which accompany this thesis.

THIS DISSERTATION
HAS BEEN MICROFILMED
EXACTLY AS RECEIVED

AVIS

La qualité de cette microfiche dépend grandement de la qualité de la thèse soumise au microfilmage. Nous avons tout fait pour assurer une qualité supérieure de reproduction.

S'il manque des pages, veuillez communiquer avec l'université qui a conféré le grade.

La qualité d'impression de certaines pages peut laisser à désirer, surtout si les pages originales ont été dactylographiées à l'aide d'un ruban usé ou si l'université nous a fait parvenir une photocopie de mauvaise qualité.

Les documents qui font déjà l'objet d'un droit d'auteur (articles de revue, examens publiés, etc.) ne sont pas microfilmés.

La reproduction, même partielle, de ce microfilm est soumise à la Loi canadienne sur le droit d'auteur, SRC 1970, c. C-30. Veuillez prendre connaissance des formules d'autorisation qui accompagnent cette thèse.

LA THÈSE A ÉTÉ
MICROFILMÉE TELLE QUE
NOUS L'AVONS REÇUE

NL-339 (r. 82/08)

Canada

THE UNIVERSITY OF ALBERTA

ORIENTATIONAL DEPENDENCE OF SURFACE ENERGY AT THE ICE-WATER INTERFACE

by

© CHRISTIE RYAN

A THESIS

SUBMITTED TO THE FACULTY OF GRADUATE STUDIES AND RESEARCH

IN PARTIAL FULFILLMENT OF THE REQUIREMENTS FOR THE DEGREE

OF Master of Science

DEPARTMENT OF Mechanical Engineering

EDMONTON, ALBERTA

FALL, 1982

Microfilming

THE UNIVERSITY OF ALBERTA

RELEASE FORM

NAME OF AUTHOR Christie Ryan

TITLE OF THESIS Orientational Dependence of Surface Energy at the Ice-Water Interface.

DEGREE FOR WHICH THESIS WAS PRESENTED Master of Science

YEAR THIS DEGREE GRANTED Fall, 1982

Permission is hereby granted to THE UNIVERSITY OF ALBERTA LIBRARY to reproduce single copies of this thesis and to lend or sell such copies for private, scholarly or scientific research purposes only.

The author reserves other publication rights, and neither the thesis nor extensive extracts from it may be printed or otherwise reproduced without the author's written permission.

(Signed) Christie Ryan

PERMANENT ADDRESS:

RR#1
Deep River, Ont
K0J 1P0

DATED July 13 1982

THE UNIVERSITY OF ALBERTA

FACULTY OF GRADUATE STUDIES AND RESEARCH

The undersigned certify that they have read, and recommend to the Faculty of Graduate Studies and Research, for acceptance, a thesis entitled Orientational Dependence of Surface Energy at the Ice-Water Interface.

submitted by Christie Ryan
in partial fulfilment of the requirements for the degree of Master of Science.

Supervisor

Date June 28 1982

Abstract

Direct solid-liquid interfacial energies are difficult to measure experimentally. A relationship between the solid-liquid surface tensions of the basal and prismatic planes of ice at -38.8°C is calculated using equilibrium thermodynamics and homogeneous nucleation theory for a nucleus shape based on that of a unit cell. Using contact angle theory and experimental data the solid-liquid surface energy for the basal plane is calculated as 17.0 dyne/cm and that of the prismatic plane as 28.9 dyne/cm.

Acknowledgement

I am particularly appreciative of my supervisor, Dr. T. Forest, whose guidance, support and unfailing patience helped me to complete this work.

I am also grateful to Brian Hirst for his assistance in the drafting and to Lois Volk for typing the thesis.

Financial support was provided by the Department of Mechanical Engineering.

Finally, special thanks to Janet and Kathleen Ryan, Janet Freeman, and Cathy Welch who gave me the emotional support that only family and good friends can.

Table of Contents

Chapter		Page
1.0	Introduction	1
2.0	Theory	8
	2.1 Equilibrium Conditions	9
	2.2 Stability Theory	26
	2.3 Expression for Equilibrium Size of Nucleus	35
3.0	Theory and Calculations	40
	3.1 Nucleation Rate Theory	43
	3.2 Calculation of Relationship of γ_1^{SL} and γ_2^{SL}	47
	3.3 Contact Angle Theory	53
4.0	Discussion	63
	4.1 Conclusions	68
References		69
Appendix I: Properties of Water		73
Appendix II: Geometric Relationship of Area in Cyrstal		74

List of Tables

Table		Page
1.1	Estimates of γ^{SL} Based on Nucleation Experiments.....	5
1.2	Estimates of γ^{SL} Based on Theories.....	5
1.3	Estimates of γ^{SL} Based on Experimental Measurement...	6
1.4	Estimates of γ^{SL} Based on Crystal Growth Experiments.	6

List of Figures

Figure		Page
1.1	Wilhelmy Plate Method.....	3
2.1	Single-Component Films A and B.....	10
2.2	Variation of a Property in the Surface Layer.....	12
2.3	Single-Component Films A and B.....	15
2.4	Thermodynamic Equilibrium of a Solid Nucleus.....	19
2.5	Growth of One Face of a Crystal.....	21
2.6	Formation of a Solid Nucleus in a Liquid Volume.....	27
2.7	The Variation of Helmholtz Free Energy with Radius..	32
2.8	Theoretical Nucleus Shape Consisting of Planar Surfaces.....	34
2.9	Phase Diagram for a Typical Liquid that Expands on Freezing.....	37
2.10	Phase Diagram Illustrating Cooling Process at Constant Pressure.....	39
3.1	Phase Diagram of the Solid Phases of Water.....	41
3.2	Shape of Unit Cell for Hexagonal Ice.....	42
3.3	Relationship Between Water Droplet Size and Homogeneous Nucleation Temperature.....	45
3.4	Relationship Between the Surface Tensions of the Basal (γ_1^{SL}) and Prismatic (γ_2^{SL}) Planes of Ice.....	50
3.5	Effect of Varying the Assumed Rate at Which Nuclei are Formed on	51
3.6	Three Phases in Equilibrium with Each Other.....	53
3.7	Three Phase, Two Component System.....	55
3.8	Contact Angle for Carbon Disulfide on Basal Plane of Ice.....	59

Figure Page

3.9 Diagram of Proposed Ice Crystal Nucleus..... 62

4.1 Variation of Liquid-Solid Interfacial Surface Tension for the Basal Plane of Ice with Temperature..... 65

List of Symbols

A	area
a	slope of straight line
b	y-intercept of straight line
c	concentration
F	Helmholtz free energy
h	Planck's constant
h_α	perpendicular distance to face α from centre of nucleus
I_h	hexagonal ice
J	number of nuclei formed per unit volume per unit time
K	Boltzmann's constant
L	latent heat of fusion
N	mole number
n	number of moles per unit volume
O	point defined by Wulff's equation
P	pressure
R	radius
S	entropy
T	temperature
U	internal energy
V	volume
u	unit volume
Z	rate constant

α arbitrary index

β arbitrary index

γ surface tension

ξ dummy variable

η dummy variable

μ chemical potential

λ liquid-solid pressure difference

θ_e equilibrium contact angle

π pi

Γ adsorption

1.0 Introduction

The surface energy of an interface is the work required to create a unit area of the interface. The following four surface energies can be defined for any liquid-solid-vapour system.

1. γ^{LV} - the liquid-vapour interfacial tension,
2. γ^{SV} - the solid-vapour interfacial tension,
3. γ^{SL} - the solid-liquid interfacial tension,
4. γ^{gb} - the grain boundary energy.

In this work the system considered is an ice-water-water vapour system and values for γ^{SL} the solid-liquid interfacial tensions are calculated.

The solid-liquid interfacial tension is important to many processes. The temperatures at which solids nucleate, whether it be on foreign particles as in heterogeneous nucleation, or by the spontaneous growth of water molecules combining together to form an ice nucleus, homogeneous nucleation, are largely determined by the liquid-solid interfacial tension. The morphology of crystal growth, particle engulfment, frost heave and pipeline freezing are all examples of phenomena where surface tension has a critical role.

Of the previously defined surface energies only the liquid-vapour surface energy is relatively easy to measure. The Wilhelmy plate method is one well-documented method (Davies and Rideal, 1963). Essentially the

method measures the additional pull on a thin plate when it becomes partially submerged (see Figure 1.1). The additional force is equal to the product of the perimeter of the plate and the surface tension. Other common methods include the small ring method, the sessile drop method, the drop weight method and pendant drop method, all of which are documented by Matijevic (1969:101-152). The liquid-vapour interfacial tension for water-water vapour is calculated in chapter three of this work.

The ice-water vapour interfacial tension is more difficult to measure and estimates for this value vary. Mason (1952) and McDonald (1953) calculated the number of hydrogen bonds that must be broken to create an ice surface. At $0^{\circ}C$ their estimates for γ^{SV} range from 85-112 dyne/cm. Ketchum and Hobbs (1969) used a direct experimental method involving measurement of dihedral contact angles and calculated a value of 109 ± 3 dyne/cm. These values for γ^{SV} must be considered average values since they are not specific to a particular plane of ice.

Methods for measuring γ^{SL}, the solid-liquid surface tension are numerous and varied. Homogeneous nucleation theory (explained in more detail in chapter three) and experiments are used by many researchers to estimate this value. Turnbull (1950) was one of the first to use homogeneous nucleation theory to calculate the interfacial energy of solid nuclei and their corresponding liquids.

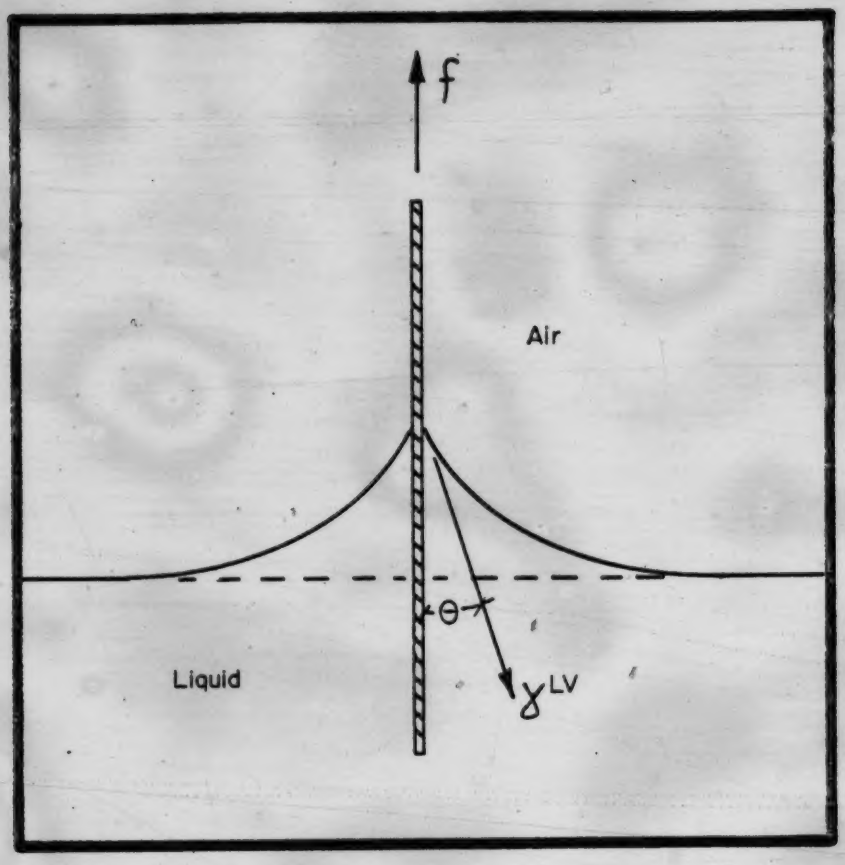

Figure 1.1 Wilhelmy Plate Method

The pull on a verticle plate per unit perimeter is $\gamma^{LV} \cos \theta$. (Adapted from Davies and Rideal, 1963:46)

A summary of Turnbull's and other experimenters' estimates for γ^{SL} is given in Table 1.1. Other methods include theoretical estimates, Table 1.2, direct measurements of grain boundary groove,[1] measurement of dihedral and contact angles, Skapski's capillary cone method (Table 1.3) and crystal growth experiments (Table 1.4). As seen from Tables 1.1 to 1.4, the values for γ^{SL} for ice-water vary from 6 to 50 dyne/cm. Note that only Hillig (1958) and Simpson et al (1974 a and 1974 b) report any orientational dependence for the surface tension. Although Hesstvedt (1967) realized that each different kind of face on a solid nucleus should have a unique value for surface tension, he did not calculate them. He incorporates a geometric factor which varies for different crystal shapes into his equations. The value he obtains is thus a weighted mean. The approach adapted in this work is definitive because it maintains the identity of the surface tensions corresponding to different faces of the solid nucleus. Since "ice generally crystallizes in hexagonal prisms, this form is usually taken to be the form of the germ" (nucleus) (Dufour-Defay, 1963:162). In the following chapters, a nucleus shape based on the 'unit cell' for ice is used, ie a hexagonal prism. It is important to

---

[1] When a crystalline solid is exposed to a vapour or liquid grain boundary grooves form at the interface. Measurement of the grain boundary groove angle, the use of Young's equation (see chapter three) and experimental data for γ^{LV} permits the calculation of γ^{VS} and γ^{LS} (see Hobbs, 1974)

Table 1.1 Estimates of γ^{SL} Based on Nucleation Experiments

(Adapted from Kallungal (1975:62)

Reference	dyne/cm
Wood & Walton (1970)	$27.53 \pm .037$
Turnbull (1950)	32.1
Carte (1959)	16.0
Jacobi (1955)	15.5
Hesstvedt (1964)	31.7

Table 1.2 Estimates of γ^{SL} Based on Theories (Kallungal (1975:61)

Reference	dyne/cm
Defour & Defay (1963)	10-49
Fletcher (1959)	20
Turnbull (1965)	38-50
Skapski (1956)	27.8

Table 1.3 Estimates of γ^{SL} Based on Estimated Measurements (Adapted from Kallungal (1978:62)

Reference	dyne/cm
Jones (1973)	44 ± 10
Jones and Chadwick (1971)	41 ± 9
Ketchum & Hobbs (1969)	33 ± 3
Suzuki & Kuroiwa (1975)	45 ± 15
Jones (1970)	46
Skapski (1957)	44 ± 10

Table 1.4 Estimates of γ^{SL} Based on Crystal Growth Experiments (Adapted from Kallungal 1975:63)

Reference	dyne/cm
Fernandez (1967 a)	31.8 ± 1.8
Poisot (1968)	49.3
Vlahakis (1972)	33.2 ± 4
Hardy, Coriell and Sekerka (1971)	25.0
Hardy and Coriell (1968)	16.0
Kotler and Taishis (1968)	20 ± 2
Simpson et al (1974 a)	28.0 (prismatic plane)
Simpson et al (1974 b)	6.24 (basal plane)
Hillig (1958)	6.4 (basal plane)

note that only the shape of the unit cell is chosen, not the relative size. For example the nucleus could be flat and disk-like or long and columnar. Equilibrium theory is used to define each surface tension in terms of the measurable quantities temperature and pressure. Stability analysis will be used to illustrate the concept of a "critical size" nucleus for a given temperature and pressure. Homogeneous nucleation rate theory and experimental data are used to generate a relationship between the surface tensions for the different planes of the nucleus. To calculate the individual values of the surface tensions, recent work on contact angle theory and experiments are used to calculate the solid-liquid surface tension of the basal crystallographic planes of ice.

2.0 Theory

This chapter develops the theory necessary to arrive at an expression for the equilibrium size of a solid nucleus surrounded by a liquid in terms of the measurable quantities of temperature, T, and pressure, P. The postulatory formulation of reversible thermodynamics, as treated by Callen (1960) is utilized to analyze the thermodynamic equilibrium and a solid nucleus in a surrounding liquid. The chapter is divided into the following 3 subsections:

2.1) Equilibrium Conditions.

2.2) Stability Theory.

2.3) Expression for Equilibrium Size of Nucleus.

2.1 Equilibrium Conditions

In this section the conditions under which a solid nucleus is in thermodynamic equilibrium with its liquid phase are developed. The agreement of predictions of equilibrium thermodynamics with our intuitive conceptualizations of temperature and pressure are often illustrated (Callen, 1960). Unfortunately this cannot be said for surface tension. Therefore the opportunity to illustrate that the behaviour of the partial differential of internal energy with respect to area agrees with our intuitive notions of surface tension is taken.

To illustrate the agreement of equilibrium thermodynamics to our intuitive concept of surface tension, the system shown in Figure 2.1 is considered. Single component films A and B each float on an inert liquid. They are separated by a movable inert barrier. The system is in equilibrium at constant, uniform temperature. The energy minimum principle states that dU_T, the total internal energy change for the system is zero:

$$dU_T = 0. \tag{2.1.1}$$

The internal energy, U^s, for the surface layers A and B is a function of the entropy, S^s, the area, A^s, and the number of moles of material, N^s, in the surface layer:

$$U^s = U^s(S^s, A^s, N^s) \tag{2.1.2}$$

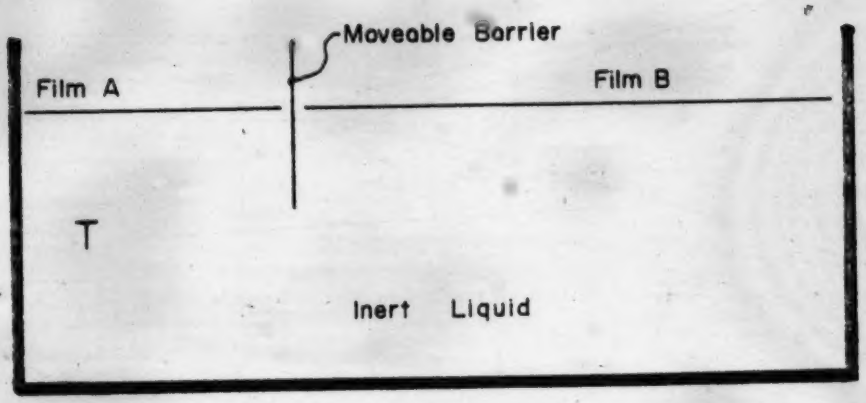

Figure 2.1 Single-Component Films A and B.

When any two phases are in contact with each other they are separated by an interfacial layer see Figure 2.2. The value of a given property will vary continuously from its value in the liquid phase to that in the solid phase. In the system to be discussed in the following pages the surface layer is replaced by a dividing surface.

At this surface there is a discontinuity in the value of the property. This is a conceptualization conceived by Gibbs (1961) while studying the phenomena of capillarity. The position of this dividing surface is defined as being where the adsorbtion of component one, "the solvent", is zero where

$$\Gamma_1 = \frac{N_1^s}{A} . \qquad (2.1.3)$$

The quantities U^s, N^s, S^s are commonly known as 'excess properties' in that they represent the difference between the total amount of property and the amounts in the liquid (') and solid (") phases.

They are commonly defined as follows:

$$U^s = U - U' - U'' \qquad (2.1.4)$$

$$S^s = S - S' - S'' \qquad (2.1.5)$$

and

$$N_i^s = N_i - N_i' - N_i'' \qquad (2.1.6)$$

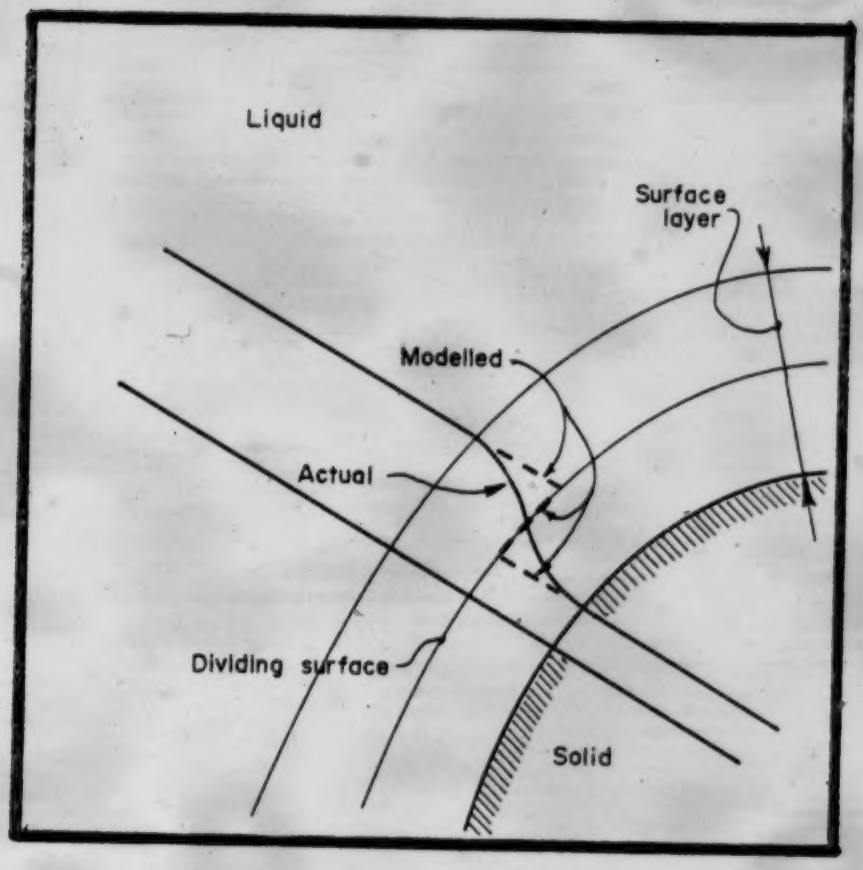

Figure 2.2 Variation of a Property in the Surface layer.

———actual variation
-----modelled variation

Applying equation 2.1.2 to the system in Figure 2.1 yields:

$$dU^s_A + dU^s_B = \left(\frac{\partial U^s_A}{\partial S^s_A}\right)_{A^s_A, N^s_A} dS^s_A + \left(\frac{\partial U^s_B}{\partial S^s_B}\right)_{A^s_B, N^s_B} dS^s_B + \left(\frac{\partial U^s_A}{\partial A^s_A}\right)_{S^s_A, N^s_A} dA^s_A +$$

$$\left(\frac{\partial U^s_B}{\partial A^s_B}\right)_{S^s_B, N^s_B} dA^s_B + \left(\frac{\partial U^s_A}{\partial N^s_A}\right)_{S^s_A, A^s_A} dN^s_A + \left(\frac{\partial U^s_B}{\partial N^s_B}\right)_{S^s_B, N^s_B} dN^s_B , \quad (2.1.7)$$

In equation 2.1.7 the partial differentials are more commonly known as the following intensive parameters:

$$\left(\frac{\partial U}{\partial S}\right)_{A,N} \equiv T \quad \text{temperature,} \quad (2.1.8)$$

and $\left(\frac{\partial U}{\partial N}\right)_{S,V} \equiv \mu$, the chemical potential. (2.1.9)

The following discussion illustrates how the partial differential, $(\partial U/\partial A)_{S,N}$, behaves in a manner associated with γ , the surface tension.

The following constraints are evident:

1) $$dN^s_A = 0; \quad (2.1.10)$$

2) $$dN^s_B = 0; \quad (2.1.11)$$

3) $$S^s_A + S^s_B = \text{constant}, \quad (2.1.12)$$

implying $$dS^s_A = -dS^s_B ; \quad (2.1.13)$$

4) $$A^s_A + A^s_B = \text{constant}, \quad (2.1.14)$$

implying $$dA^s = -dA^s_B . \quad (2.1.15)$$

Using equations 2.1.1 and 2.1.8 to 2.1.15 to simplify equation 2.1.7 yields:

$$(T_A - T_B)\, dS_A^s = \left(\left(\frac{\partial U_A^s}{\partial A_A^s} \right)_{S_A^s, N_A^s} - \left(\frac{\partial U_B^s}{\partial A_B^s} \right) \right) dA_A^s = 0. \qquad (2.1.16)$$

The variables dS_A^s and dA_A^s must be permitted to vary independently of each other. This leads to the two equilibrium conditions:

$$T_A = T_B \qquad (2.1.17)$$

and

$$\left(\frac{\partial U_A^s}{\partial A_A^s} \right)_{S_A^s, N_A^s} = \left(\frac{\partial U_B^s}{\partial A_B^s} \right)_{S_B^s, N_B^s} \qquad (2.1.18)$$

Physically, at equilibrium, the surface tensions, γ_A and γ_B, are expected to be equal; just as the quantities in equation 2.1.18 are equal.

To examine the effect of a perturbation on the system, consider the effect of imposing a greater surface tension of film A than film B on the system illustrated Figure 2.1. This state of the system will be referred to as state 1 and the equilibrium state will be referred to as state 2.

Figure 2.3 is an illustration of state 1. Note that the temperatures of films A and B are equal, only the surface tension has been altered.

The total energy U, for each state is:

$$U^{(1)} = U_A^{(1)} + U_B^{(1)} \qquad (2.1.19)$$

and

$$U^{(2)} = U_A^{(2)} + U_B^{(2)} \qquad (2.1.20)$$

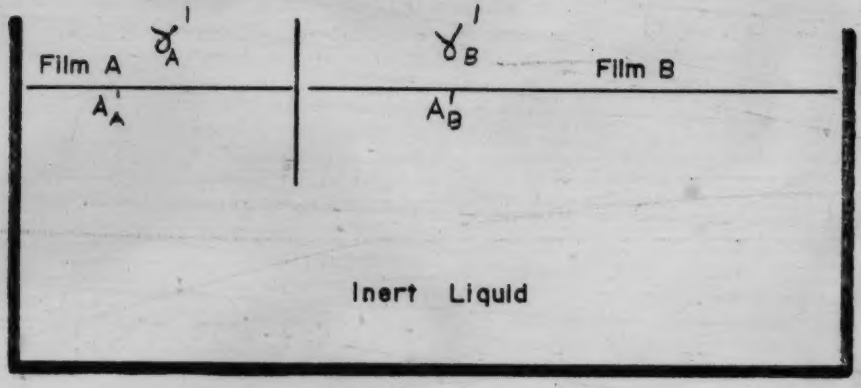

Figure 2.3 Single-Component Films A and B, where $\gamma_A^{(1)}$ is greater than $\gamma_B^{(1)}$.

The change in energy, ΔU, between states 1 and 2 is

$$\Delta U \equiv U^{(2)} - U^{(1)} . \tag{2.1.21}$$

Substituting equations 2.1.19 and 2.1.20 into equation 2.1.21 yields:

$$\Delta U = (U_A^{(2)} - U_A^{(1)}) + (U_B^{(2)} - U_B^{(1)}) . \tag{2.1.22}$$

A Taylor series expansion about the equilibrium point, state 2, exclusive of terms higher than first order yields:

$$U_A^{(1)} = U_A^{(2)} + \left(\frac{\partial U^{(1)}}{\partial A_A}\right)_{(2)} (A_A^{(1)} - A_A^{(2)}) + \dots , \tag{2.1.23}$$

$$U_B^{(1)} = U_B^{(2)} + \left(\frac{\partial U^{(1)}}{\partial A_B}\right)_{(2)} (A_B^{(1)} - A_B^{(2)}) + \dots , \tag{2.1.24}$$

These can be simplified to:

$$(U_A^{(2)} - U_A^{(1)}) = -\gamma_A^{(1)} \Delta A_A , \tag{2.1.25}$$

and

$$(U_B^{(2)} - U_B^{(1)}) = -\gamma_B^{(1)} \Delta A_B . \tag{2.1.26}$$

Substituting equations 2.1.25 and 2.1.26 into equation 2.1.22 yields:

$$\Delta U = \gamma^{(1)} \Delta A_A^{(1)} - \gamma^{(1)} \Delta A_B . \tag{2.1.27}$$

Recalling constraint 2.1.14 and substituting into equation 2.1.27 yields the following expression:

$$\Delta U = -(\gamma_A^{(1)} - \gamma_B^{(1)}) \Delta A_A^{(1)} . \tag{2.1.28}$$

The energy minimum principle implies that ΔU is a negative quantity.

Since $(\gamma_A^{(i)} - \gamma_B^{(i)})$ is imposed as being a positive quantity, $\Delta A_A^{(i)}$, must be a positive quantity. This is in agreement with our intuitive feeling that the film A with a greater surface tension increases the area it occupies at the expense of film B. Physically it is expected that the film with the larger surface tension will expand its area.

In a laboratory situation intensive parameters are often the most readily varied. It is simpler to measure an intensive parameter like temperature than it is to measure S, the entropy. The partial Legendre transform that replaces temperature for entropy as the independent variable in the energy representation is the Helmholtz free energy, F. The Helmholtz free energy is a function of temperature, volume and mole fractions $N_1, N_2 \ldots N_r$:

$$F = F(T, V, N_1, N_2, \ldots N_r) \tag{2.1.29}$$

The complete differential, dF, is,

$$dF = -S\,dT - P\,dV + \mu_i\,dN_i \quad i = 1, 2, \ldots r \tag{2.1.30}$$

The equilibrium condition in the Helmholtz free energy representation is:

"The equilibrium value of any unconstrained internal parameter in a system in diathermal contact with a heat reservoir

minimizes the Helmholtz potential at constant temperature (equal to that of the heat reservoir)" (Callen 1960:105).

Thus $$dF = 0, \qquad (2.1.31)$$

subject to the auxiliary condition that

$$T = T^r \qquad (2.1.32)$$

where T^r is the reservoir temperature. The Helmholtz free energy is the representation that is most convenient for the forthcoming discussion of a solid nucleus in equilibrium with a liquid.

Consider, now, the thermodynamic equilibrium of a solid nucleus, assumed to be under hydrostatic stress, as shown in Figure 2.4, surrounded by a liquid, each phase, including interfacial zone, consisting of a finite number, r, of non-reacting components. This system is isolated by a heat bath to maintain a constant temperature. The total volume, V, which is held constant, is the sum of the nucleus volume, V'', and the liquid volume, V'. The volume of liquid phase is far greater than that of the solid phase nucleus making changes of pressure due to growth or dissolution of the solid nucleus negligible. As mentioned earlier, under these constraints the appropriate potential to express the equilibrium condition is the Helmholtz free energy, equation 2.1.30. The condition of equilibrium for this system is that the total change of free energy must equal zero,

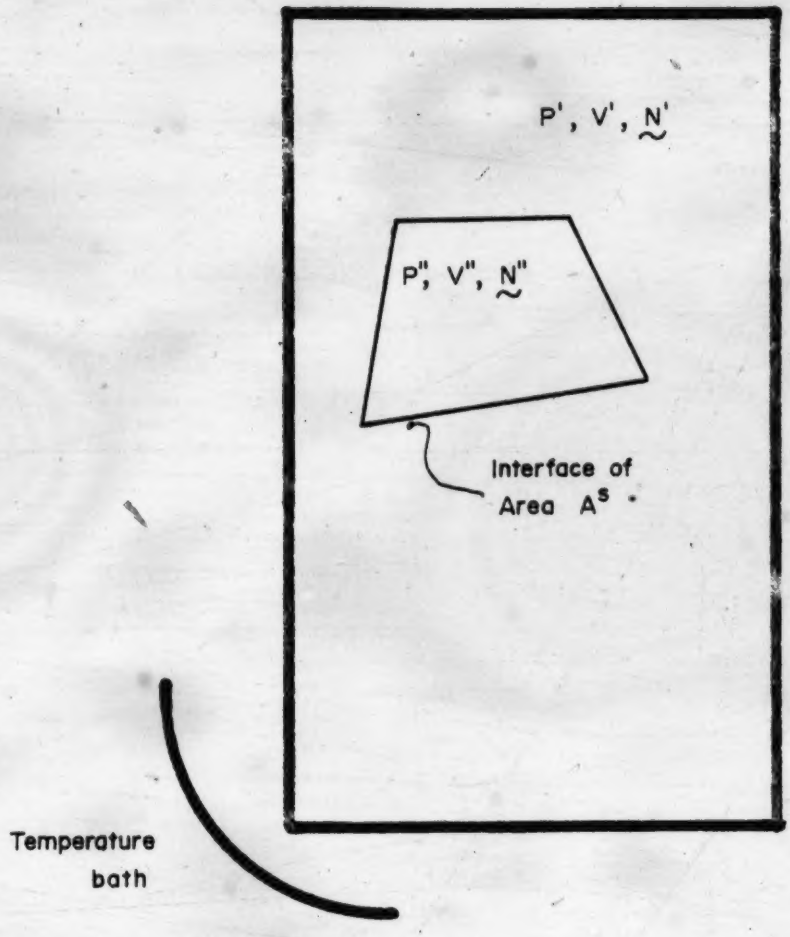

Figure 2.4 Thermodynamic Equilibrium of a Solid Nucleus

where
(') denotes liquid phase
(") denotes solid phase
(s) denotes interface.

$$dF)_{T,V,\underset{\sim}{N}} = 0 \qquad (2.1.33)$$

where $\underset{\sim}{N}$ denotes the mole numbers, of each component, N_1, N_2, ..., N_r. This equilibrium condition is subject to the following constraints:

i) the total volume is constant, ie.

$$V' + V'' = V \qquad (2.1.34)$$

ii) the total number of moles of each component is constant

ie $$N_i' + N_i'' + \sum_{\alpha} N_{i,\alpha}^{s} = \text{constant} \quad i = 1, 2 \ldots r \qquad (2.1.35)$$

To maintain the generality of the problem it is assumed that the solid nucleus has α plane[1] surfaced sides. Figure 2.5 represents the growth of one such plane. A_β is the area of this particular face, h_β is the perpendicular distance from the face to the centre of the nucleus. V_*'' is the original volume of the solid nucleus and dV'' is the volume of the addition to face A_β. V' is the volume of the liquid and dV' (the volume of liquid solidified) is considered to be negligible compared to the total volume of liquid.

The total change in the Helmholtz free energy is the sum of the change in the free energy of the bulk phases and the change in free energy of the surface, ie:

$$dF = dF' + dF'' + dF^{s} + dF_*'' \qquad (2.1.36)$$

[1] This paper will be restricted to plane surfaces.

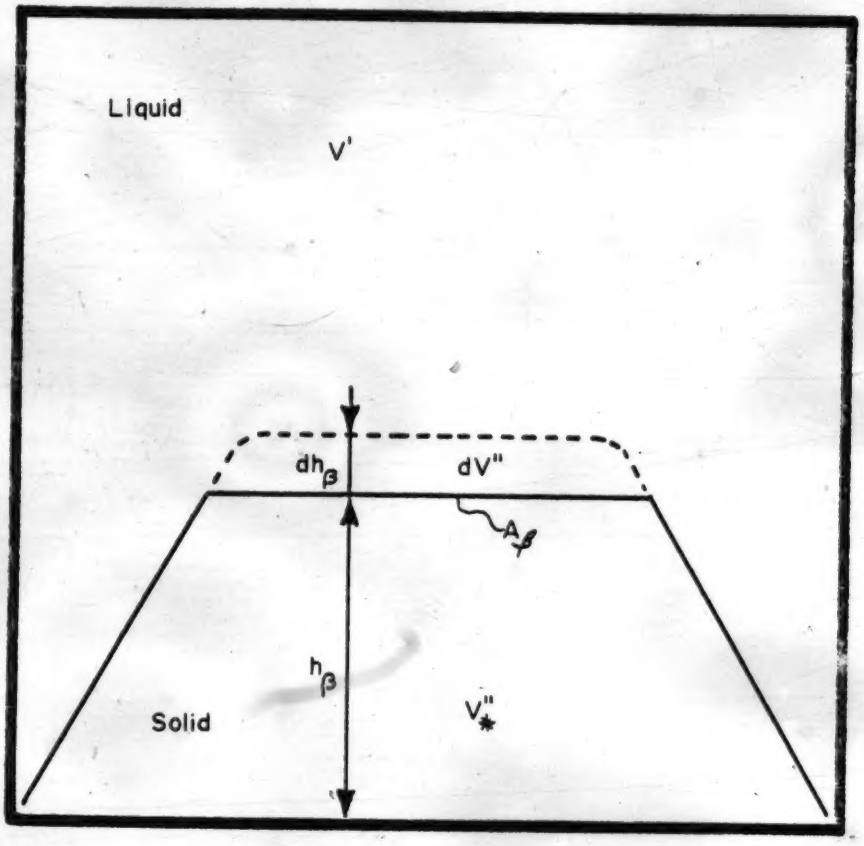

Figure 2.5 Growth of One Face of a Crystal (Adapted from Defay and Prigogine, 1966)

The change in free energy of the fixed volume V_*'' is zero.

Therefore $$dF_*'' = 0. \qquad (2.1.37)$$

The first term in equation 2.1.36, dF', is the change of free energy in the volume V';

$$dF_*' = -P'dV' + \sum_{i=1}^{r} \mu_i' dN_i', \qquad (2.1.38)$$

where μ_i' is the chemical potential of the i^{th} component and dN_i' is the change in the number of moles of the i^{th} component in the volume V'.

The change in free energy due to the change of phase of the volume dV'' is

$$dF'' = -P''dV'' + \sum_{i=1}^{r} \mu_i'' dN_i''. \qquad (2.1.39)$$

dF^s, the change in free energy for α, planar surfaces is

$$dF^s = \sum_{\alpha} \gamma^{\alpha} dA^{\alpha} + \sum_{i,\alpha} \mu_{i,\alpha}^{s} dN_{i,\alpha}^{s}. \qquad (2.1.40)$$

Using the relationship,

$$dV' + dV'' = 0. \qquad (2.1.41)$$

substituting equations 2.1.37 to 2.1.40 into equation 2.1.36 and re-arranging the terms yields:

$$dF = -(P'' - P')dV'' + \sum_{\alpha=1}^{s} \gamma^{\alpha} dA^{\alpha} + \sum_{i=1}^{r} (\mu_i' dN_i' + \mu_i'' dN_i'' + \sum_{\alpha=1}^{s} \mu_{i,\alpha}^{s} dN_{i,\alpha}^{s}). \qquad (2.1.42)$$

The energy minimum principle, equation 2.1.33, with constraint equations 2.1.34 and 2.1.35 applied to equation 2.1.42 gives two distinct sets of equilibrium conditions: one involving surface tensions and the other chemical potentials.

Since moles and volume must be able to vary independently it is possible to divide equation 2.1.42 into the following two equations:

$$-(P''-P')\,dV'' + \sum_{\alpha=1}^{s} \gamma^{\alpha}\, dA^{\alpha} = 0, \tag{2.1.43}$$

and $$\sum_{i=1}^{r} \left(\mu_i'\, dN_i' + \mu_i''\, dN_i'' + \sum_{\alpha=1}^{s} \mu_{i,\alpha}^{s}\, dN_{i,\alpha}^{s} \right) = 0. \tag{2.1.44}$$

The following discussion will first treat equation 2.1.43 and then equation 2.1.44.

From Figure 2.5 the following geometric relationship is evident:

$$dV'' = A_{\beta}\, dh_{\beta}. \tag{2.1.45}$$

Substituting equation 2.1.45 into equation 2.1.43 yields:

$$-(P''-P')A_{\beta}\, dh_{\beta} + \sum_{\alpha=1}^{s} \gamma^{\alpha}\, dA^{\alpha} = 0. \tag{2.1.46}$$

From geometrical considerations it can be shown that;

$$A_{\beta} = 1/2 \sum_{\alpha} h^{\alpha} \frac{dA^{\alpha}}{dh_{\beta}}. \tag{2.1.47}$$

Substituting equation (2.1.47) into equation (2.1.46) and collecting terms gives:

$$\left(-\lambda/2 \sum_{\alpha} h^{\alpha} + \sum_{\alpha} \gamma^{\alpha}\right) \frac{dA^{\alpha}}{dh_{\beta}} = 0, \qquad (2.1.48)$$

where $$\lambda \equiv (P'' - P') . \qquad (2.1.49)$$

For a particular face α the solution to this equation is

$$\gamma^{\alpha} = \lambda/2 \; h^{\alpha} . \qquad (2.1.50)$$

This form of solution is known as the Wulff equation (Defay and Prigogine, 1966:296),

$$\frac{\gamma_1}{h_1} = \frac{\gamma_2}{h_2} = \frac{\gamma_3}{h_3} = \ldots \quad \frac{\lambda}{2} \qquad (2.1.51)$$

It can be shown (Defay and Prigogine, 1966:296) that "in every crystal which is in equilibrium there exists a point 0 such that the Wulff relations are satisfied. The Wulff form is therefore the only equilibrium form" 0, is defined as the point for which the distance of each face from 0 is proportional to the surface tension of that face.

Return to equation 2.1.44 to determine the second set of equilibrium conditions. Differentiating equation 2.1.35 yields:

$$dN_i' = -\left(\sum_{\alpha} dN_{i,\alpha}^{s} + dN_i''\right)_{i=1,2\ldots r} \qquad (2.1.52)$$

Substituting 2.1.52 into equation 2.1.44 gives,

$$dN_i''(\mu_i'' - \mu_i') + \sum_{\alpha}\left(dN_{i,\alpha}^{s}(\mu_{i,\alpha}^{s} - \mu_i'')\right) = 0 \qquad (2.1.53)$$
$$i=1,2\ldots r$$

Since dN_i'' and $\sum_\alpha dN_{i,\alpha}^s$ cannot equal zero.

$$\mu_i'' = \mu_i' = \sum_\alpha \mu_{i,\alpha}^s \qquad (2.1.54)$$

Thus the chemical potentials of all three phases are equal.

2.2 Stability Analysis

For the purpose of stability analysis a system of r components with a spherical nucleus will be considered to make the analysis simpler. Consider the two systems illustrated in Figures 2.6(a) and 2.6(b). The system in state A is a large volume of liquid solution at pressure, P^1, surrounded by a heat bath at temperature, T. The system shown in figure 2.6(b) is a spherical solid nucleus which is close to its' equilibrium state. The nucleus has a hydrostatic pressure P_β'' . The radius R, of the nucleus is close to the equilibrium radius, R_c. The total number of moles in the nucleus, $\underset{\sim}{N}''$, is close to the number of moles in the critical nucleus.

The difference in free energy between the systems is

$$\Delta F = F_\beta - F_A , \tag{2.2.1}$$

where

$$F_A = F_A' \tag{2.2.2}$$

and

$$F_\beta = F_\beta' + F_\beta'' + F_\beta^s . \tag{2.2.3}$$

In state A

$$F_A = -P_A' V_A' + \sum_{i=1}^{r} \mu_{iA}' N_{iA}' . \tag{2.2.4}$$

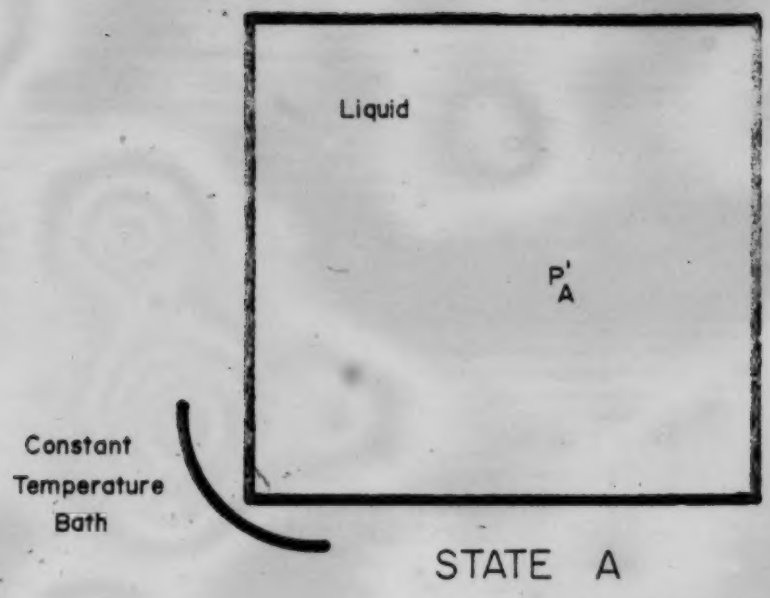

Figure 2.6(a)

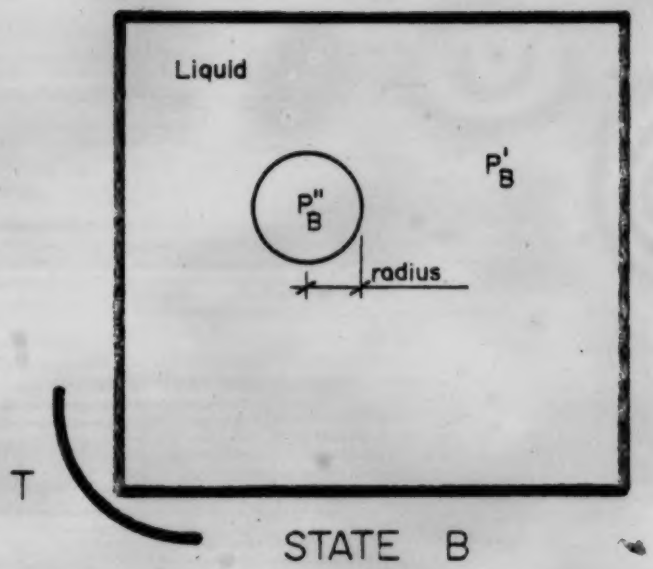

Figure 2.6(b)

Figure 2.6 Formation of a Solid Nucleus in a Liquid Volume

where
(') denotes liquid phase
('') denotes solid phase

For state B sufficiently close to equilibrium[1], the Helmholtz free energy can be expressed as

$$F_B = -P_B' V_B' - P_B'' V_B'' + \sum_{i=1}^{r} \left(\mu_{B,i}' N_{B,i}' + \mu_{B,i}'' N_{B,i}'' + \mu_{B,i}^{s} N_{B,i}^{s} \right) + \gamma A \qquad (2.2.5)$$

The system in states A and B is constrained by the following two relationships:

$$V_A' = V_B' + V_B'' \qquad (2.2.6)$$

and

$$N_{A,i} = N_{B,i}' + N_{B,i}'' + N_{B,i}^{s} \quad i = 1, 2 \ldots r. \qquad (2.2.7)$$

The pressure in state A, P_A', is not significantly different than that in state B, P_B', because the nucleus is small relative to the volume of the surrounding liquid. Since the pressure, concentrations and temperature of the bulk liquid phases in states A and B are constant, the chemical potentials are also constant:

$$\mu_i' = \mu_i'(P, T, c_i) \quad i = 1, 2 \ldots r. \qquad (2.2.8)$$

---

[1] Assume that each small mass element is in a state of local equilibrium for which properties are the same function of the local macroscopic variables as at the equilibrium state. "This assumption of local equilibrium is not in contradiction with the fact that the system as a whole is out of equilibrium" as long as "the dissipative processes are sufficiently dominant to exclude large deviations from statistical equilibrium." (Glandorff and Progogine, 1971)

It is also assumed that the number of moles in the interfacial zone is much smaller than the number of moles in either the bulk liquid phase or the solid nucleus. Thus the following three relationships are evident:

$$P_B' - P_A' \simeq 0, \tag{2.2.9}$$

and

$$\mu_{B,i}' - \mu_{A,i}' \simeq 0, \tag{2.2.10}$$

$$N_{B,i}^s \simeq 0 \qquad i = 1, 2 \ldots r; \tag{2.2.11}$$

Substituting equations 2.2.4 and 2.2.5 into 2.2.1 yields

$$\Delta F = -(P_B' - P_A')V_B' - (P_B'' - P_A')V_B'' + \gamma A +$$

$$\sum_{i=1}^{r}\left[(\mu_{B,i}' - \mu_{A,i}')N_{B,i}' + (\mu_{B,i}'' - \mu_{A,i}')N_{B,i}'' + (\mu_{B,i}^s - \mu_{A,i}')N_{B,i}^s\right]. \qquad i = 1, 2 \ldots r. \tag{2.2.12}$$

Equations 2.2.9, 2.2.10, and 2.2.11 are used to simplify equation 2.2.12 to

$$\Delta F = -\Delta P V_B'' + \Delta\mu_i N_{B,i} + \gamma A^s \qquad i = 1, 2 \ldots r, \tag{2.2.13}$$

where

$$\Delta P = P_B'' - P_A', \tag{2.2.14}$$

and

$$\Delta\mu_i = \mu_{B,i}'' - \mu_{A,i}' \qquad i = 1, 2 \ldots r, \tag{2.2.15}$$

Both ΔP and $\Delta\mu$ $(i = 1, 2, \ldots r)$ are developed for the near equilibrium state.

Expanding ΔP and $\Delta \mu$ about the equilibrium state using a Taylor series yields:

$$\Delta P(R, N''_{B,i}) = \Delta P(R_c, N''_{c,i}) + \frac{\partial \Delta P}{\partial R}\Big|_{R_c, N''_{c,i}} \Delta R + \frac{\partial \Delta P}{\partial N''_{B,i}} \cdot \Delta N''_{B,i} + \dots , \quad i = 1,2 \dots r. \tag{2.2.16}$$

where $$\Delta R = R - R_c \tag{2.2.17}$$

and $$\Delta N''_{B,i} \equiv (N''_{B,i} - N''_{c,i}) \quad i = 1,2 \dots r \tag{2.2.18}$$

and

$$\Delta \mu_i(R, N''_{B,i}) = \Delta \mu(R_c, N''_{c,i}) + \frac{\partial \Delta \mu_i}{\partial R}\Big|_{R_c, N''_{c,i}} \Delta R + \frac{\partial \Delta \mu_i}{\partial N''_{B,i}}\Big|_{R_c, N''_{c,i}} \Delta N''_{B,i} \quad i = 1,2 \dots r \tag{2.2.19}$$

State B is considered to be sufficiently close to the equilibrium size nucleus that only zero order terms in equations 2.2.16 and 2.2.19 need be retained.

At equilibrium Laplace's[1] capillary equation (Defay and Prigogine, 1966) is used to relate the pressure, radius and surface tension of a spherical nucleus. From equation 2.1.54.

$$\Delta \mu_i(R_c, N_{c,i}) = 0 \quad i = 1,2 \dots r \tag{2.2.20}$$

For a spherical nucleus the volume and surface area can be expressed in terms of the radius R, which is near the critical radius, R_c:

$$V = 4/3 \pi R^3 \tag{2.2.21}$$

and

$$A = 4 \pi R^2 \tag{2.2.22}$$

[1] $p'' - p' = 2\gamma/R_c$

Substituting Laplace's equation 2.1 and equations 2.2.20 to 2.2.22 into equation 2.2.13 yields

$$\Delta F = 4\gamma\pi R^2[1-(2/3)\,R/R_c]. \qquad (2.2.23)$$

A plot of this function is shown in figure 2.7 At R=R the free energy, ΔF, is an extremum. At the critical size the conditions of equilibrium are satisfied. It is obvious from the plot of this function that the critical nucleus is unstable. A nucleus whose radius is smaller than R_c will completely dissolve and a nucleus larger than the critical size will spontaneously grow. This theoretical result has been confirmed for the liquid-gas bubble equilibrium (Tucker and Ward, 1975). The implication of this is that there is an energy barrier, equal to ΔF_{max}, to the nucleation process. This is the energy required to form a nucleus of at least critical size. For a spherical nucleus, $R = R_c$

$$\Delta F_{max} = 4/3\,\gamma\pi R_c^2. \qquad (2.2.24)$$

This expression can be extended to form an equation for ΔF_{max} for a multifaceted nucleus in the following way. Substitute equation 2.2.20 into equation 2.2.13 to yield

$$\Delta F = -\Delta P V_B'' + \gamma A^s. \qquad (2.2.25)$$

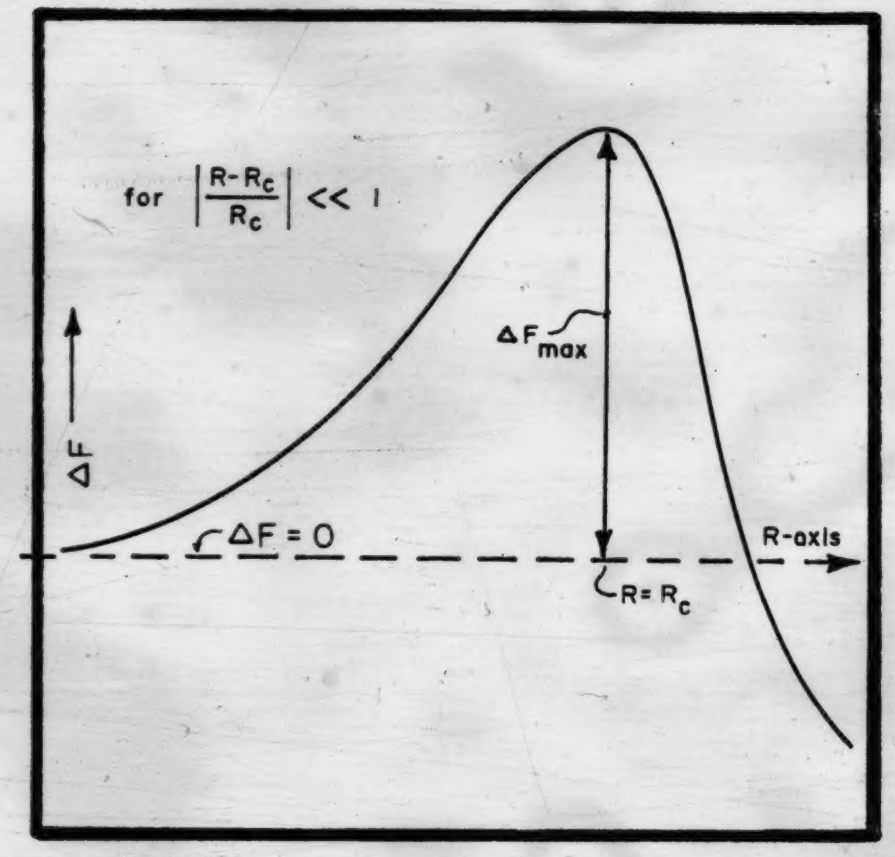

Figure 2.7 The Variation of the Change In Helmholtz Free Energy with Radius

If the crystal is assumed to consist of α planar surfaces, (see fig. 2.8), γA^s can be expressed as the sum of α surfaces of the nucleus:

$$\gamma A^s = \sum_{\alpha} \gamma^{\alpha} A^{\alpha} \qquad (2.2.26)$$

Similarly it is possible to divide the volume V into α pyramids. The total volume is then

$$V = \sum_{\alpha} (1/3) A^{\alpha} h^{\alpha} \qquad (2.2.27)$$

The change in pressure, ΔP, is

$$\Delta P = (2\gamma^{\alpha})/h^{\alpha} \qquad (2.2.28)$$

for each crystal face α. The change in free energy, obtained by substituting equations 2.2.26 to 2.2.28 into equation 2.2.25 is equal to:

$$\Delta F_{max} = -\sum_{\alpha} (1/3) A^{\alpha} h^{\alpha} \cdot \frac{2\gamma^{\alpha}}{h^{\alpha}} + \sum_{\alpha} \gamma^{\alpha} A^{\alpha} \qquad (2.2.29)$$

Equation 2.2.29 can be further simplified to

$$\Delta F_{max} = \sum_{\alpha} (1/3) \gamma^{\alpha} A^{\alpha} \qquad (2.2.30)$$

This relationship will be important in section 3,1 concerning nucleation theory.

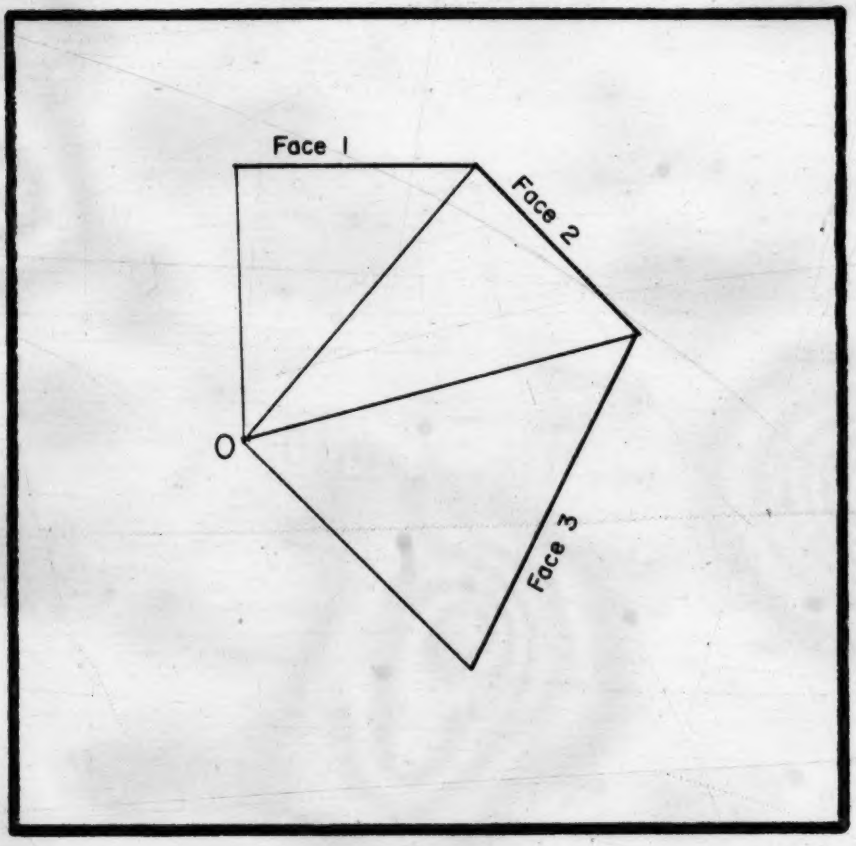

Figure 2.8 Theoretical Nucleus Shape Consisting of Planar Surfaces

2.3 Expression for Equilibrium Size of Nucleus

It is now important to derive an expression for the equilibrium size of the nucleus in terms of the measurable quantities temperature and pressure. The system described in section 2.2 will be used with the additional restriction that it consist entirely of one component. At equilibrium

$$\mu'(T, P') = \mu''(T, P''), \tag{2.3.1}$$

where

$$\mu''(T, P'') = \mu''(T, P') - v''(P''-P'). \tag{2.3.2}$$

Substituting equation 2.3.1 into equation 2.3.2 yields

$$\mu'(T, P') = \mu''([illegible], P') - v''(P''-P). \tag{2.3.3}$$

T_o, the bulk equilibrium freezing temperature, is that temperature for which

$$\mu''(T_o, P') = \mu'(T_o, P'). \tag{2.3.4}$$

The chemical potentials in equation 2.3.3 can be expressed in terms of T by using the Gibbs-Duhem relation:

$$\mu(T, P) = \mu(T_o, P) - \int_{T_o}^{T} s\,dT \tag{2.3.5}$$

Thus

$$\mu'(T, P') = \mu'(T_o, P') - \int_{T_o}^{T} s'\,dT \tag{2.3.6}$$

and

$$\mu''(T, P') = \mu''(T_o, P') - \int_{T_o}^{T} s''\,dT \tag{2.3.7}$$

Substituting equations 2.3.6 and 2.3.7 into equation 2.3.3 and using the equality 2.3.4 yields:

$$-\int_{T_0}^{T}(s'-s'')dT = v''(p''-p') \qquad (2.3.8)$$

The latent heat of fusion, L, is defined as,

$$L \equiv T(s'-s'') . \qquad (2.3.9)$$

Substituting equation 2.3.9 into equation 2.3.8 yields

$$-\int_{T_0}^{T}(L/T)\,dT = v''(p''-p') \qquad (2.3.10)$$

Let $\langle L \rangle$ be the average latent heat over the temperature range T_0 to T and assume that (L/T) is not strongly dependent on temperature. Integrating equation 2.3.10 over the temperature range T_0 to T yields:

$$(p''-p') = \langle L \rangle \ln(T_0/T)/v'' . \qquad (2.3.11)$$

Substituting this value of Δ P into equation 2.2.28 yields:

$$h^{\alpha} = 2\gamma v''/(\langle L \rangle \ln(T_0/T)) . \qquad (2.3.12)$$

where h^{α} is the equilibrium distance of face α from point O. Note that h^{α} is a function of temperature and pressure, the pressure dependence entering via the dependence of T_0 on pressure. This is evident in Figure 2.9 which is a phase diagram of a substance that expands on solidification. As the pressure increases, the temperature at which the phase

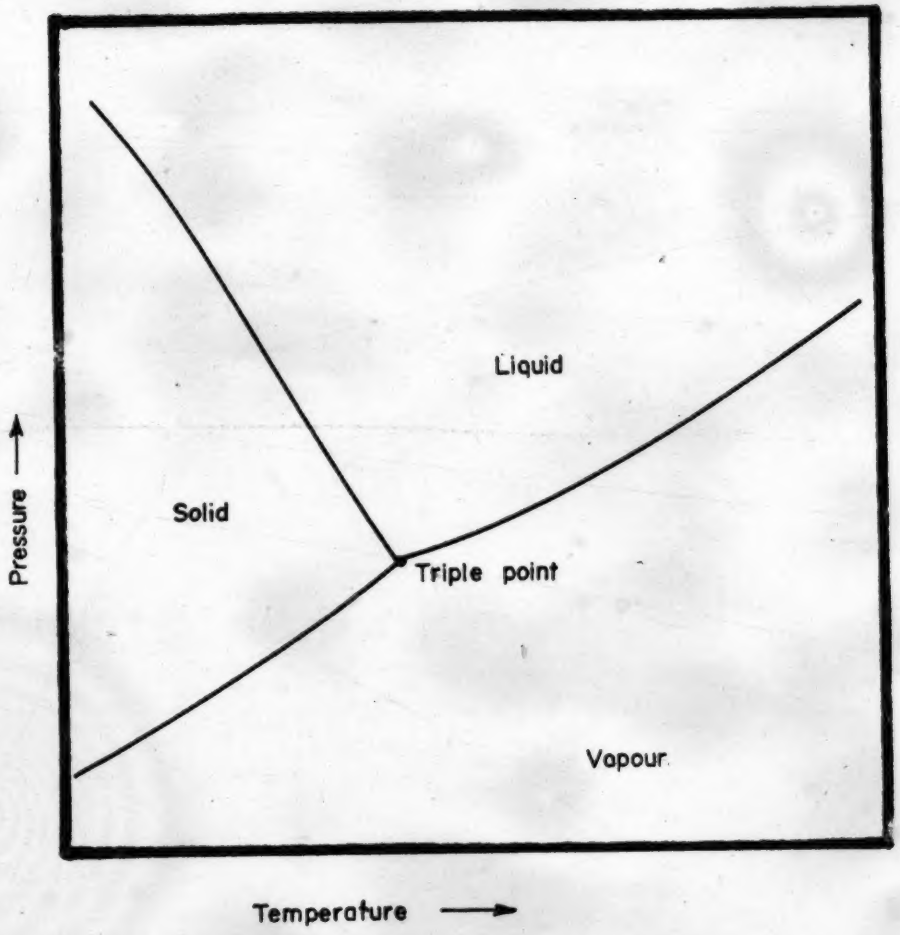

Figure 2.9 Phase Diagram for a Typical Liquid that Expands on Freezing.

transition occurs increases as well. L depends on pressure to a lesser extent.

Figure 2.10 is a phase diagram for a typical cooling process at constant pressure. Liquid at pressure P can be cooled to point A, the bulk freezing point, and all points along this curve are in stable equilibrium states. The portion of the curve from A to B, the spinodal point, is metastable. That is, the system will remain in the original state as long as no large property perturbations occur. Microscopically the substance is always fluctuating in density and if a disturbance large enough to take a portion of the system to state D occurs that part of the system will remain as state D. This implies that there is a critical size of a nucleus. The smallest amount of material that remains in state D is called the critical nucleus. Under a specified temperature and pressure it is possible with nucleation theory to estimate the frequency of nucleus formation in a liquid. The next chapter will treat this subject in more detail.

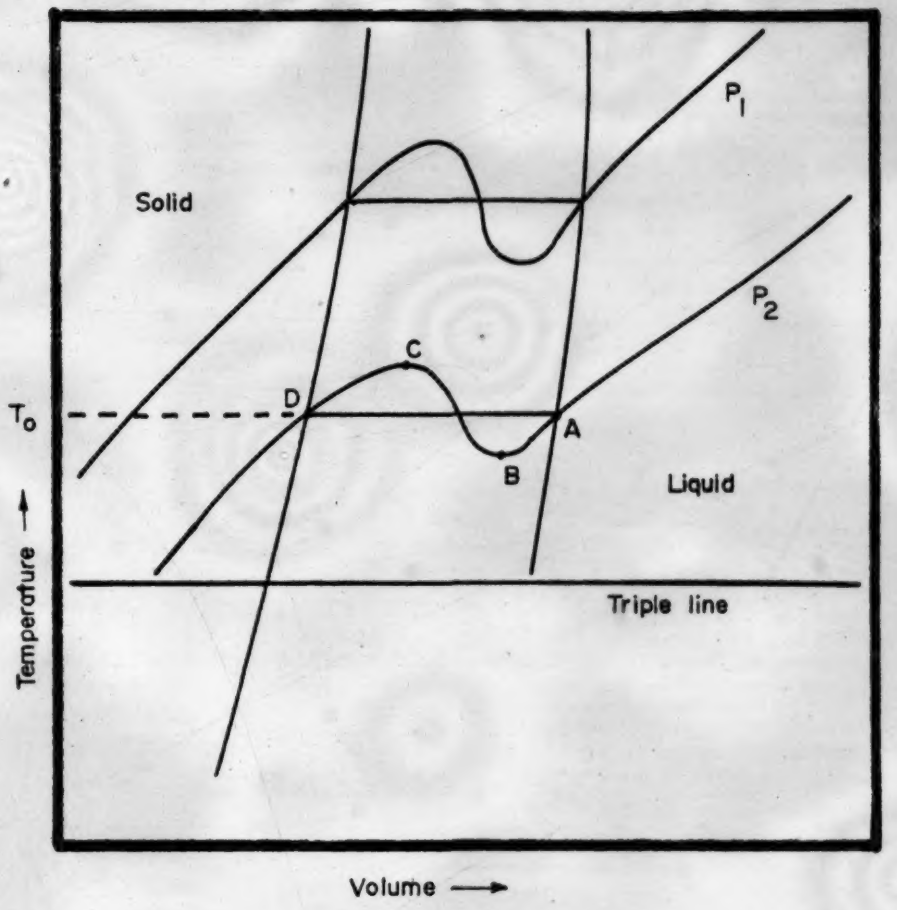

Figure 2.10 Phase Diagram Illustrating Cooling Process at Constant Pressure

3.0 Theory and Calculations

The theoretical developments derived in chapter two from equilibrium thermodynamics are applicable to any liquid-solid equilibrium. In this chapter a pure ice-water system is used to illustrate how these relationships can be used to determine the anistropic surface tensions for ice. A nucleus shape related to the shape of the unit cell is assumed. Figure 3.1, is a composite diagram of experimental observations of the shape of the unit cell at varying temperatures and pressures. From this figure, it can be seen that for ice at 1 atm and temperature between $0^{\circ}C$ and $-50^{\circ}C$ the unit cell is a hexagonal prism, commonly known as Ice I_h.

For this shape two distinct surface tensions are calculated, σ_1, corresponding to the basal surface (perpendicular to the c axis) and σ_2, corresponding to the prismatic surfaces (perpendicular to the a axis), see Figure 3.2. Using nucleation rate theory and experimental results for the maximum supercooling a relationship between the surface tensions of the two different surfaces of the water nucleus is developed. Following a short discussion of contact angle theory, experimentally obtained data for the surface energy of the basal plane of ice are used to determine unique values for σ_1 and σ_2.

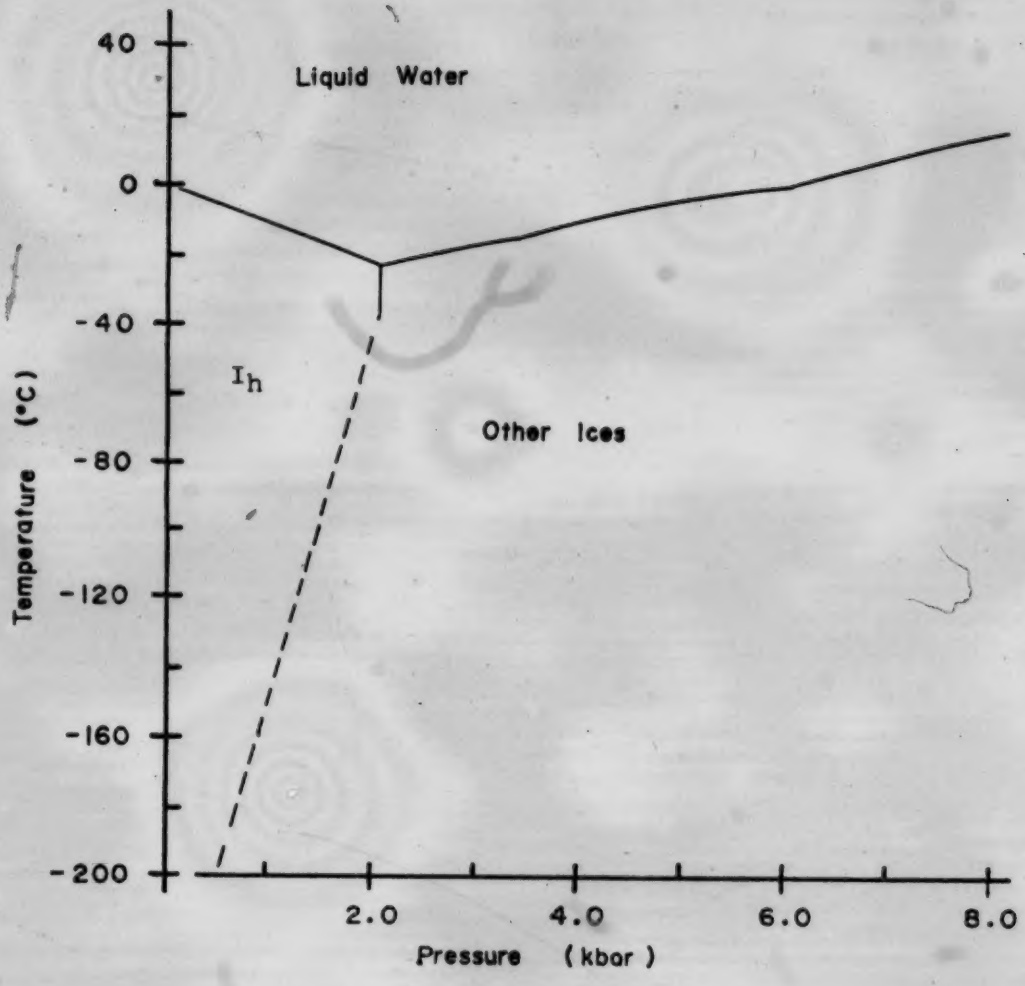

Figure 3.1 Phase Diagram of the Solid Phases of Water (adapted from Hobbs, 1974)

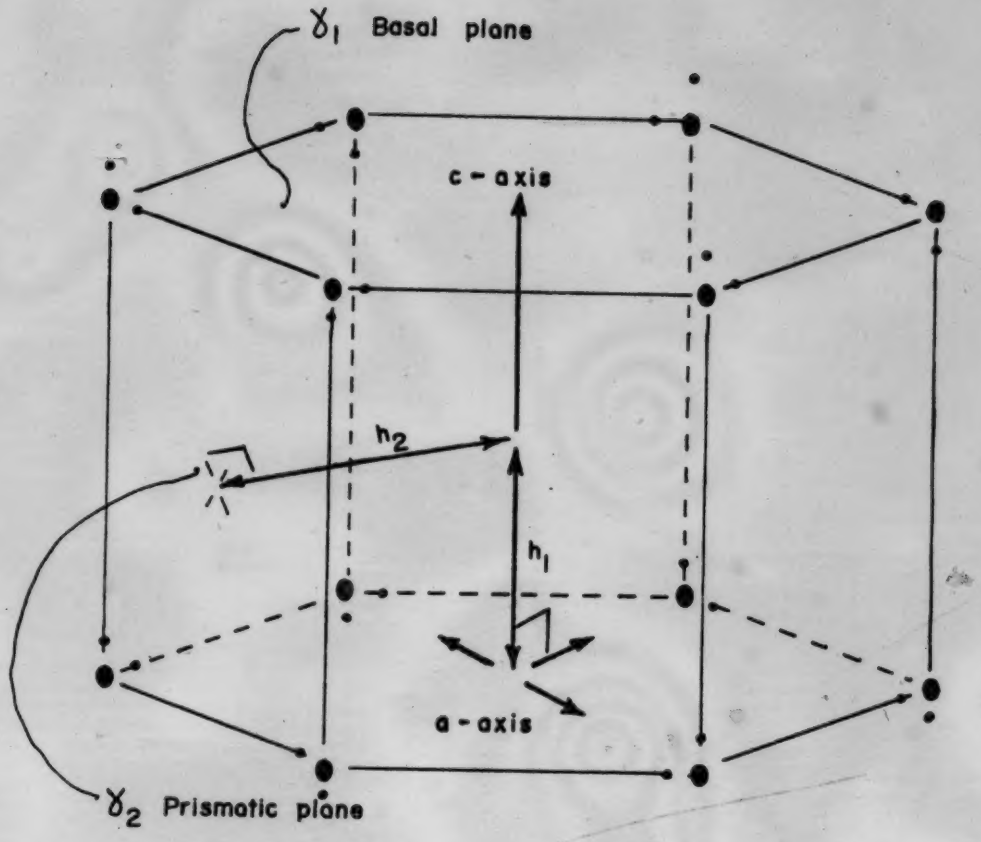

Figure 3.2 Shape of unit cell for Hexagonal Ice
Where h_1 = perpendicular distance from centroid to basal plane
h_2 = perpendicular distance from centroid to prismatic plane.

3.1 Nucleation Rate Theory

Small water droplets can be cooled well below 0°C without initiating freezing. This is because small droplets are less likely to be contaminated with foreign particles to catalyze heterogeneous nucleation. Homogeneous or spontaneous nucleation will occur as the liquid is cooled below the bulk freezing temperature (0° for water.) In supercooled water there are microscopic fluctuations in density, temperature and pressure (Frenkle, 1946). Thus tiny ice nuclei are constantly being formed. In chapter two it was shown that if a nucleus of a "critical" minimum size is created it will spontaneously grow. Since it is impossible to measure the probability of a nucleus being formed in the supercooled liquid, homogeneous nucleation theory was developed. This theory predicts the number of critical nuclei, J, which are spontaneously formed in a unit volume of liquid per unit time. Becker (1938) investigated liquid-solid systems and proposed the following form for the equation for the rate at which nuclei are formed:

$$J = Z \exp(-\Delta F/(KT)), \qquad (3.1.1)$$

where Z is the rate constant and K is Boltzmann's constant. Turnbull and Fisher (1949) expanded this theory and developed the following expression for the rate constant, Z,

$$Z = nKT/h, \qquad (3.1.2)$$

where n is the number of nuclei per unit volume and h is Planck's constant.

Turnbull (1952) generated dispersions of small droplets and used a dilatometer to experimentally demonstrate the difference between heterogeneous nucleation and homogeneous nucleation. Values for surface tension calculated by his technique are for spherical nuclei. Hesstvedt (1964) supercooled small water droplets and using homogeneous nucleation theory calculated a value of 31.7 dyne/cm for the interfacial surface tension at 0°C. Hesstvedt (1964) derived the following equation to calculate Z:

$$Z = 4/3\,\pi r^3 n K T. \qquad (3.1.3)$$

where r is the radius of the water droplet. From Figure 3.3 it is seen that a one micron water droplet will spontaneously freeze at -38.8°C. This experimentally determined maximum supercooling is assumed to be the homogenous nucleation temperature.[1] Using these values and substituting into equation 3.1.3, Z, the rate constant is 6.27×10^{24} nuclei/cm^2/s. With this value of Z, and assuming a value of J=1, ΔF_{MAX} can be expressed in terms of the critical

---

[1] This value is very close to the homogeneous nucleation temperature reported by other researchers eg: Schaefer (1948) reports -38.9°C, Schaefer (1952) reports -38.5°C, Weickman (1949) reports (-40°C).

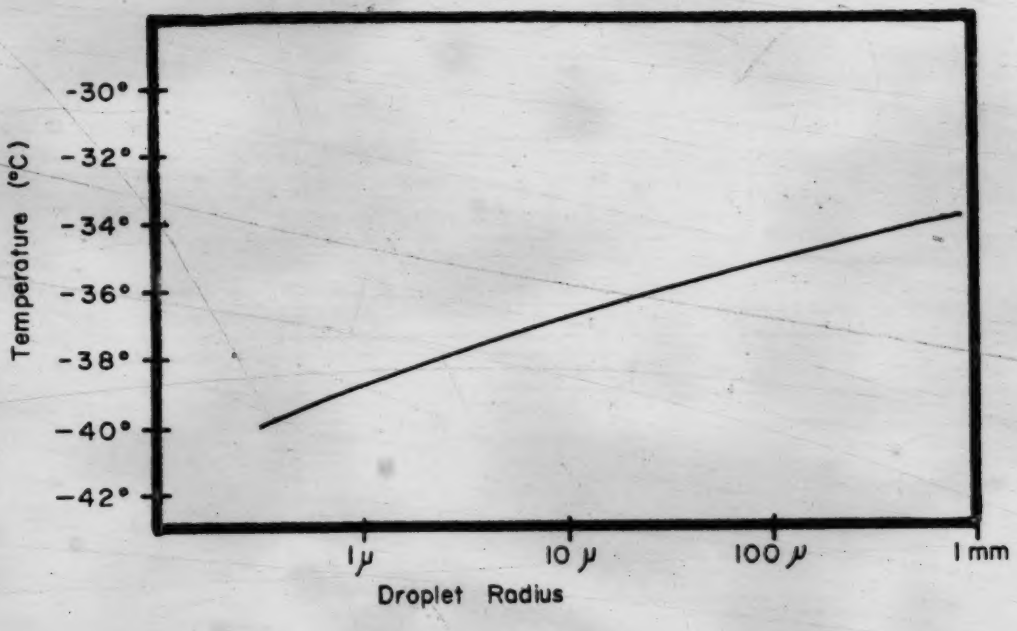

Figure 3.3 Relationship Between Water Droplet Size and Homogeneous Nucleation Temperature. (Adapted from Hesstvedt, 1964)

size based on the results in the last chapter. This equation can then be used to predict the supercooling if the surface tensions are known or (as illustrated in the following section) to predict the relationship between the surface tensions given the supercooling.

3.2 Calculation of Relationship of γ_1^{SL} and γ_2^{SL}

To calculate the relationship between γ_1^{SL} and γ_2^{SL} for the ice-water system it is necessary to assume a nucleus shape. Most researchers, like Turnbull (1950), assume that the nucleus is spherical in shape. Hesstvedt (1964) realized that unique faces of a crystal should have unique surface tensions, and that the nucleus is not necessarily spherical but he calculated a weighted mean value for different shapes. As discussed in the introduction to chapter three in this work, it will be assumed that the nucleus shape is related to the structure of the unit cell at the nucleation temperature and pressure. It is clear that the surface area of the crystal can be formulated in terms of h_1 and h_2 see Figure 3.2, the perpendicular distance from the centre of the crystal to the basal and prismatic planes, respectively. The ratios of h_1 and h_2 need not be the same as in the unit cell. Henceforward quantities subscripted as 1 refer to the basal plane and those subscripted as 2 refer to the prismatic plane.

The total area of the two basal planes, A_1, is;

$$A_1 = 12 h_2^2 \cot 60^\circ. \qquad (3.2.1)$$

The total area of the six prismatic faces, A_2, is;

$$A_2 = 24 h_1 h_2 \cot 60^\circ \qquad (3.2.2)$$

It is possible to express the distances h_1 and h_2 in terms of the surface tensions of their respective planes, γ_1^{SL} and γ_2^{SL} (as seen in chapter 2);

$$h_1 = 2\gamma_1^{SL} v'' / (\langle L \rangle \ln(T_0/T)), \quad (3.2.3)$$

and

$$h_2 = 2\gamma_2^{SL} v'' / (\langle L \rangle \ln(T_0/T)). \quad (3.2.4)$$

By substituting equations 3.2.3 and 3.2.4 for h_1 and h_2 into the area formulations, expressions relating the area to surface tension and temperature are obtained;

$$A_1 = \left[\frac{2v''}{\langle L \rangle \ln(T_0/T)}\right]^2 \cdot \cot 60^\circ \cdot 12(\gamma_2^{SL})^2 \quad (3.2.5)$$

and

$$A_2 = \left[\frac{2v''}{\langle L \rangle \ln(T_0/T)}\right]^2 \cdot \cot 60^\circ \cdot 24\gamma_1^{SL}\gamma_2^{SL} \quad (3.2.6)$$

Substituting equation 3.2.5 and 3.2.6 into equation 2.2.30 yields;

$$\Delta F_{max} = 48\gamma_1^{SL}(\gamma_2^{SL})^2 v''^2 \cot 60^\circ / (\langle L \rangle \ln(T_0/T))^2. \quad (3.2.7)$$

Equation 3.2.7 can be substituted into 3.1.1 the nucleation rate equation to give;

$$J = Z \exp\left(-48\gamma_1^{SL}(\gamma_2^{SL})^2 v''^2 \cot 60^\circ / ((\langle L \rangle \ln(T_0/T))^2 kT\right). \quad (3.2.8)$$

The exponential nature of equation 3.2.8 suggests that the relationship between γ_1^{SL} and γ_2^{SL} is relatively insensitive to the values of J and Z. For the purpose of calculation J, the nucleation rate, is set equal to 1. The rate constant

used will be the one derived from Hesstvedt (1964) in section 3.1. Solving equation 3.2.8 for $\gamma_1^{SL}(\gamma_2^{SL})^2$ using the properties of water listed in Appendix I , yields;

$$\gamma_1^{SL}(\gamma_2^{SL})^2 = 1.4 \times 10^4 (dyne/cm)^3. \qquad (3.2.9)$$

Figure 3.4 is a graph of this relationship. A graph of the percentage difference in γ_2^{SL} for two assumed values of J (J=1, and J=100) is presented in Figure 3.5. . A difference in the assumed rate of two orders of magnitude of 10 causes only a 4% difference in γ_2^{SL} . Thus it is seen that γ_2^{SL} is relatively insensitive to the assumed value of J.

In the following section unique values for γ_1^{SL} and γ_2^{SL} are determined by using contact angle theory and experimental data to arrive at a value for the surface tension of the basal plane of the ice-liquid water interface, γ_1^{SL} .

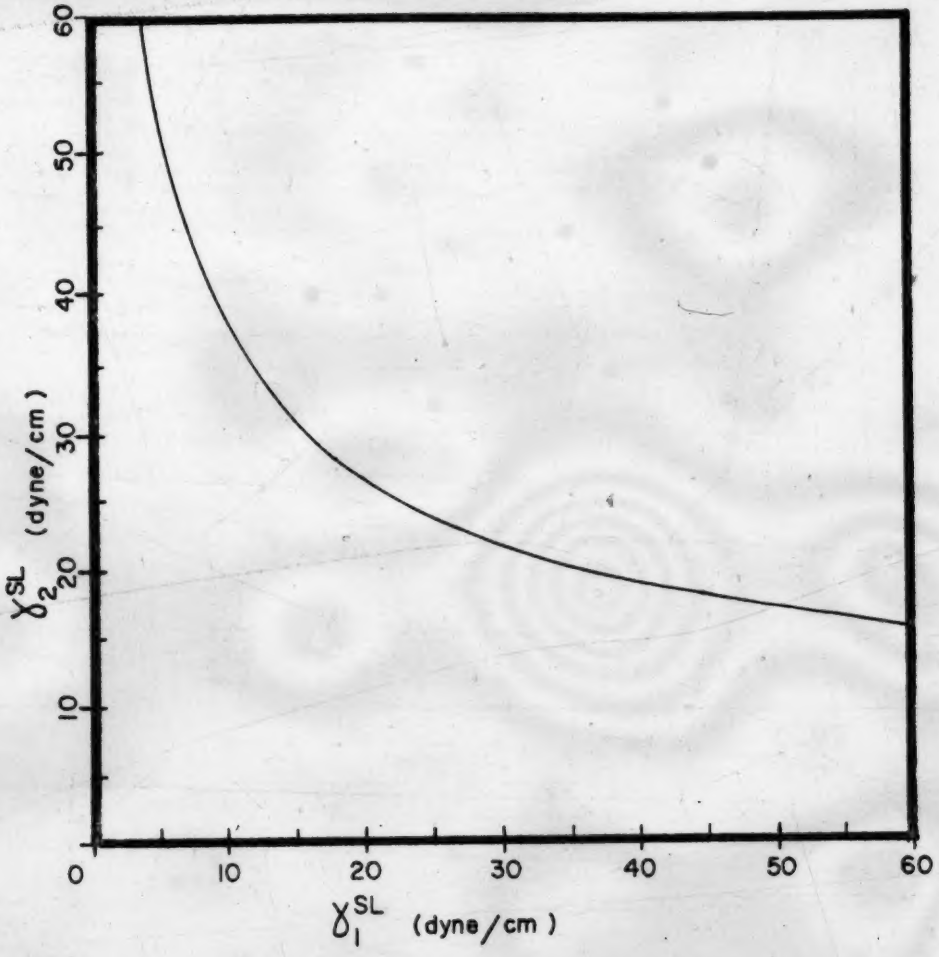

Figure 3.4 Relationship Between the Surface Tensions of the Basal, γ_1^{SL}, and Prismatic, γ_2^{SL}, Planes of Ice

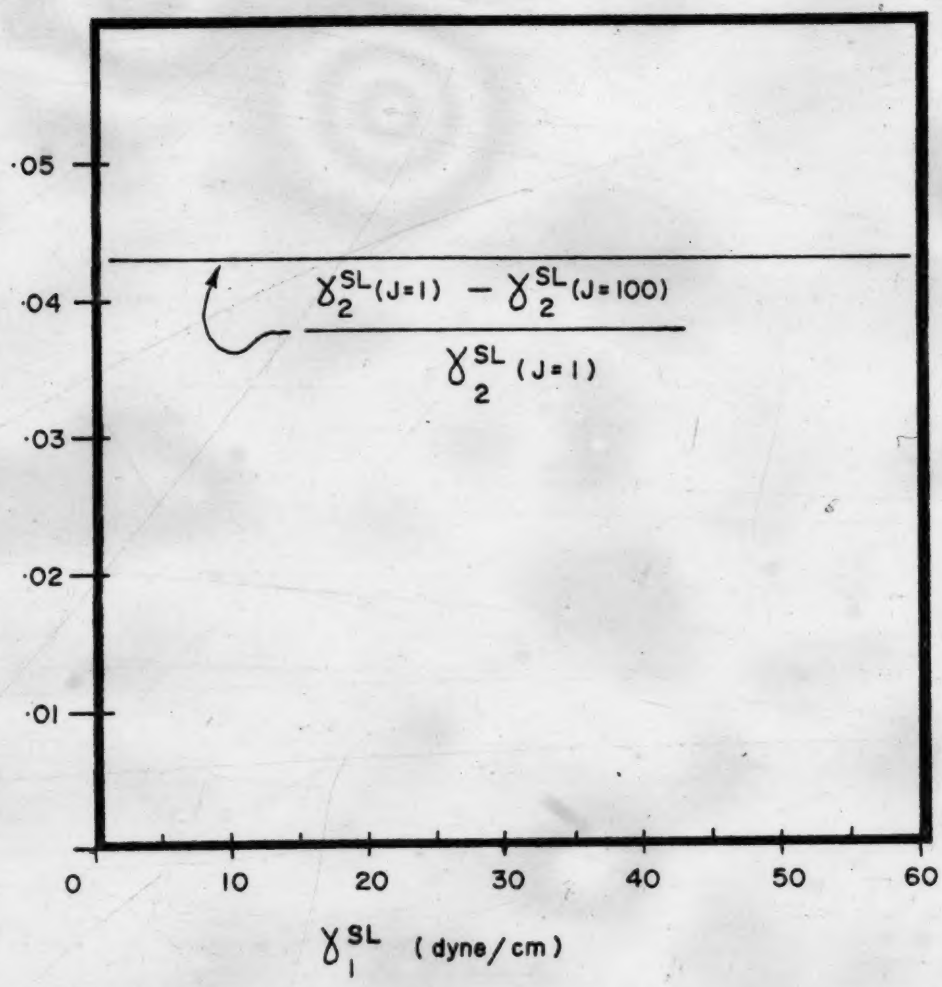

Figure 3.5 Effect of Varying the Assumed Rate at Which Nuclei are Formed on γ_2^{SL} .

3.3 Contact Angle Theory

In order to determine unique values for γ_1^{SL} and γ_2^{SL}, contact angle data for carbon disulphide (CS_2) droplets on the basal plane of ice obtained by Adamson (1970) are used. Equation of state relationships between γ^{LV}, liquid-vapour γ^{SV}, solid-vapour, and γ^{SL}, solid-liquid surface tension (Ward and Neumann, 1974) derived by Ward are used to correlate Adamson's data to the basal plane of the ice-liquid water system.

The angle at which a liquid wets a solid (Figure 3.6) when the three phases are in equilibrium is θ_e, the contact angle. The contact angle is related to the surface tensions between the three phases by Young's (1805) equation;

$$\gamma^{LV} \cos\theta_e = \gamma^{SV} - \gamma^{SL} \qquad (3.3.1)$$

Ward, (1975) states that "in any system in which a smooth, homogeneous and inert solid is in equilibrium with a liquid and a vapour phase, adsorption must take place at the solid-vapour interface and the adsorption must be positive." Whalen and Wade (1967) and Whalen (1968) measured the adsorption of liquid octaine on Teflon (contact angle 26°) and found that the solid-vapour adsorption was significant.

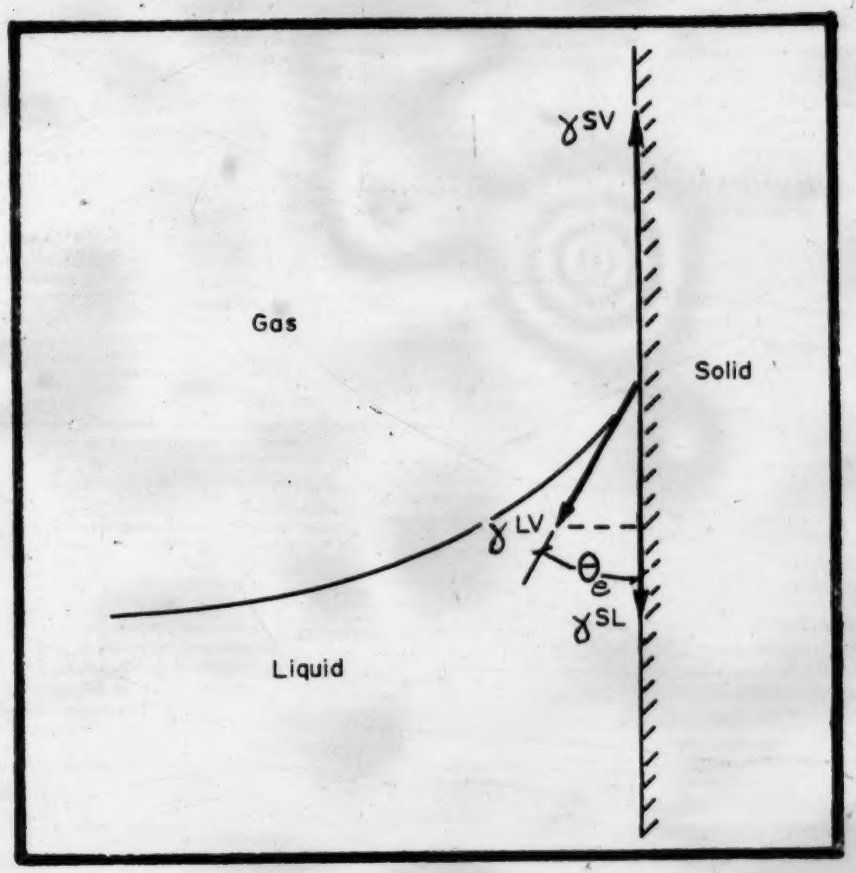

Figure 3.6 Three Phases in Equilibrium with Each Other. (Adapted from Defay and Progogine, 1966)

Using the system shown in Figure 3.7 and the following assumptions;

1. solid is non-dissolving
2. solid has negligible vapour pressure so that there is a single component present in the liquid and vapour phases.
3. solid is smooth, homogeneous and rigid,

Ward ensures that θ_e is the equilibrium contact angle. Using the method of Gibbs (1961) for equilibrium of this system,

1. uniformity of temperatures

and 2. $\mu^{LV} = \mu^{SL} = \mu^{SV}$

Ward shows that γ^{SL} is a function of γ^{SV} and γ^{LV} ie;

$$\gamma^{SL} = F(\gamma^{SV}, \gamma^{LV}) \tag{3.3.2}$$

To develop the explicit relationship of equation 3.3.2 the following derivation follows that of Ward (1975). To determine this function the following variables will be used:

$$\eta = \gamma^{LV} - \gamma^{SV} \tag{3.3.3}$$

and

$$\xi = \gamma^{LV} + \gamma^{SV} \tag{3.3.4}$$

γ^{LV} and γ^{SV} can be expressed in terms of the variables η and ξ ie;

$$\gamma^{LV} = \tfrac{1}{2}(\eta + \xi) \tag{3.3.5}$$

and

$$\gamma^{SV} = \tfrac{1}{2}(\eta - \xi) \tag{3.3.6}$$

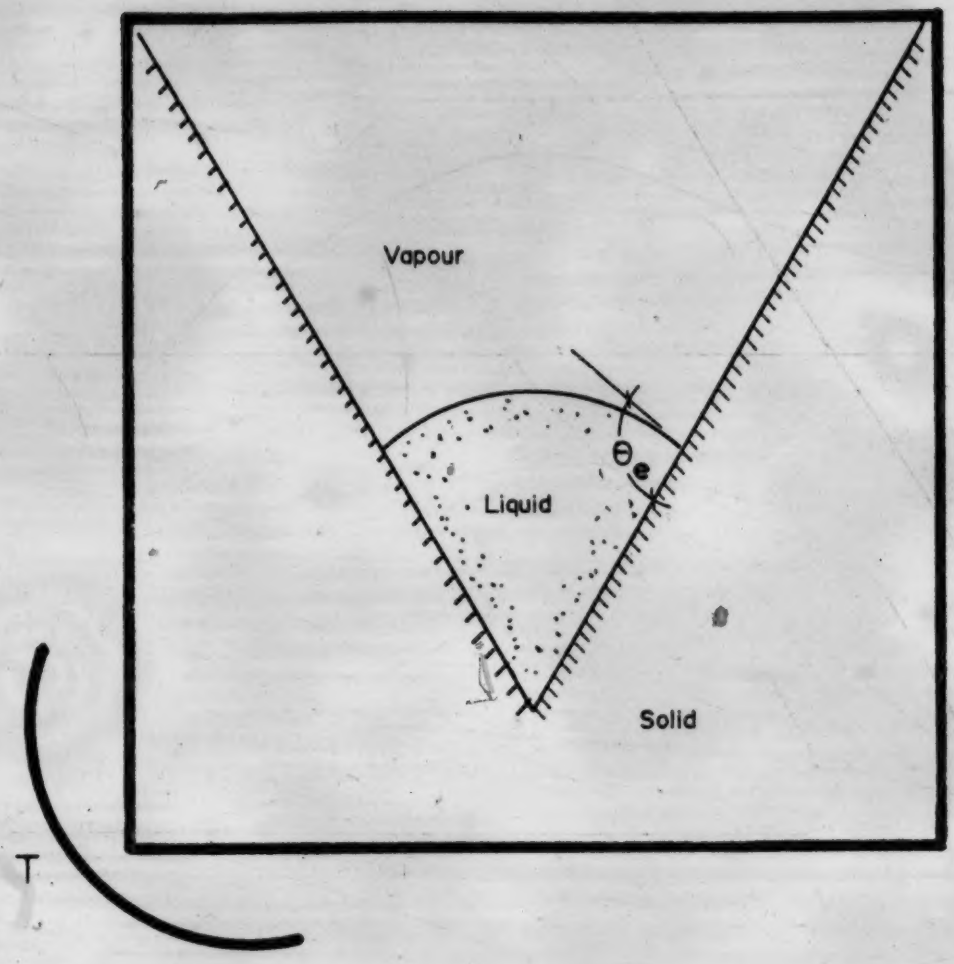

Figure 3.7 Three Phase, Two Component System
(Adapted from Ward, 1975)

Substituting equations 3.3.5 and 3.3.6 and 3.3.1 into equation 3.3.2 yields:

$$\tfrac{1}{2}(\eta - \xi) - F(\xi, \eta) = \tfrac{1}{2}((\eta + \xi)\cos\theta_e) \tag{3.3.8}$$

where γ^{SL} is a function of ξ and η because it is a function of γ^{SV} and γ^{LV}. These equations are subject to the following three limits:

1. if $\gamma^{SV} = \gamma^{LV}$ (3.3.9)

then $\cos\theta$ must equal one and therefore

$$F(\xi, 0) = 0 \tag{3.3.10}$$

2. as γ^{SV} approaches zero, θ approaches π, therefore

$$F(\eta, \eta) = \eta \tag{3.3.11}$$

3. as γ^{LV} approaches zero, and γ^{SV} remains finite, the contact angle will approach zero and therefore

$$F(-\eta, \eta) = -\eta \tag{3.3.12}$$

When adsorption is present:

$$\gamma^{SV} \simeq \gamma^{LV} \tag{3.3.13}$$

and thus

$$\eta = 0 \tag{3.3.14}.$$

Therefore, γ^{SL}, a function of ξ and η can be expanded in a Taylor series about $F(\xi, 0)$ as follows;

$$F(\xi, \eta) = F(\xi, 0) + \left(\frac{\partial F}{\partial \eta}\right)_{\eta=0} \eta + \tfrac{1}{2}\left(\frac{\partial^2 F}{\partial \eta^2}\right)_{\eta=0} \eta^2 \tag{3.3.15}$$

where higher order terms are neglected.

After defining the following functions.

$$g(\xi)=\frac{\partial F}{\partial \eta}\Big|_{\eta=0}, \tag{3.3.16}$$

and

$$f(\xi)=\tfrac{1}{2}\frac{\partial^2 F}{\partial \eta^2}\Big|_{\eta=0}, \tag{3.3.17}$$

and using equation 3.3.10, equation 3.3.15 can be written as:

$$F(\xi,\eta)=g(\xi)\eta+f(\xi)\eta^2 \tag{3.3.18}$$

Since equation 3.3.18 must also satisfy the limits of 3.3.11 and 3.3.12,

$$g(\xi)=0 \tag{3.3.19}$$

and

$$f(\xi)=1/\xi \tag{3.3.20}$$

Substituting back into equation 3.3.2 yields the following equation:

$$\gamma^{SL}=(\gamma^{LV}-\gamma^{SV})^2/(\gamma^{LV}+\gamma^{SV}) \tag{3.3.21}$$

Equation 3.3.21 is the equation of state in the presence of adsorption. Equation 3.3.21 can be combined with equation 3.3.1 to yield another relationship which will be useful in the following analysis.

$$\gamma^{SV}=(\gamma^{LV}+\gamma^{LV}\cos\theta)/(3-\cos\theta) \tag{3.3.22}$$

In the following paragraphs, a value of γ^{SV} (basal plane of ice - CS_2 vapour) is obtained using the previously developed contact angle equations and Adamson's data. This value of γ^{SV} is assumed to be approximately equal to γ^{SV} (basal plane of ice-water vapour).

Experimental evidence indicates that the solid-vapour interfacial tension is not strongly dependent on the adsorption of the contacting vapour or the liquid-vapour surface tension. From contact angle data Hellwig and Neumann (1968) found that γ^{SV} the solid-vapour surface tension is nearly constant for various fluids on a solid.

The equation of state is then used to calculate γ^{SL} (basal plane of ice-liquid water). Knowing γ^{SL} for the basal planes of ice, γ^{SL} for the prismatic planes can be calculated.

Figure 3.8 is a graph of the contact angles that Adamson (1970) measured for different temperatures of liquid carbon disulphide on the basal plane of ice. At -38.8°C the contact angle for ice is about 29°C. A linear regression for CS_2 liquid vapour surface tension yielded the following equation:

$$\gamma^{LV} = 74.98\,(1. - T/549.)^{1.12} \qquad (3.3.23)$$

Using Adamson's data, and equations 3.3.22 and 3.3.23, γ^{SV}, the surface tension for the basal plane of ice - CS_2 vapour is calculated. At the measured supercooling of -38.8°C, the calculated value for γ^{SV} is 36.1 dyne/cm.

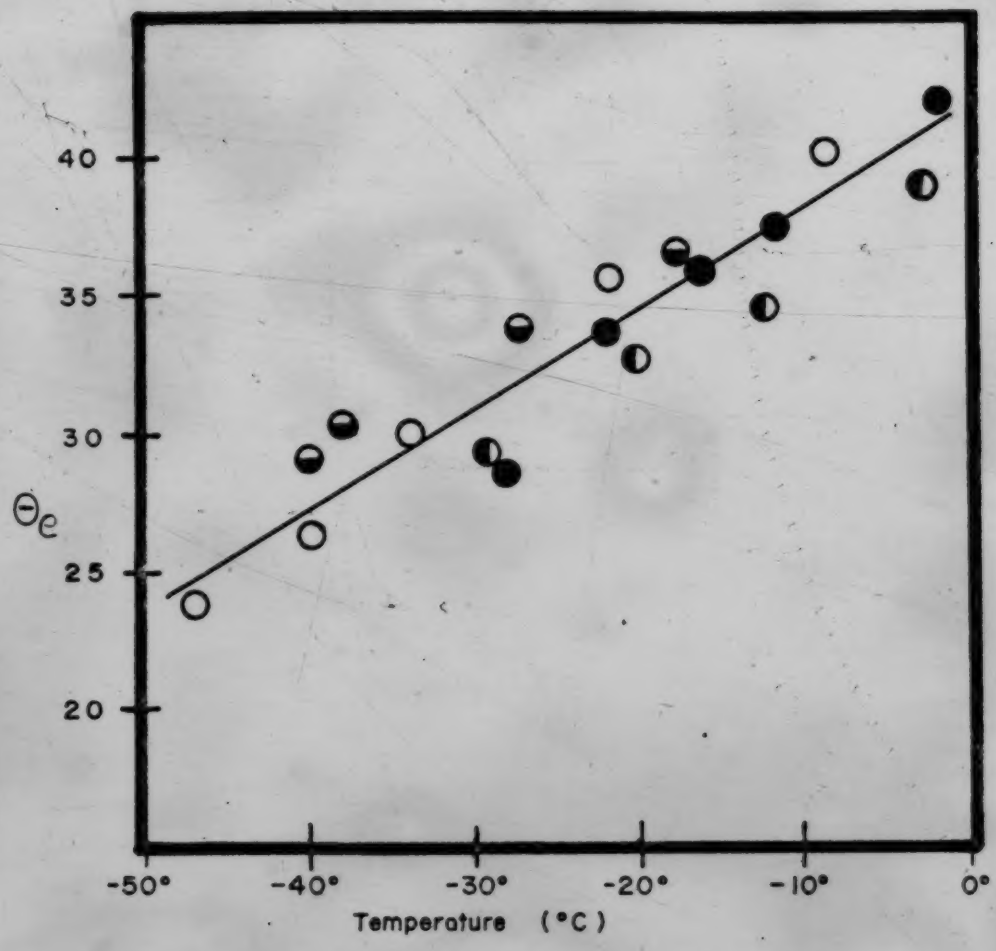

Figure 3.8 Contact Angle for Carbon Disulfide on Basal Plane of Ice.
(Adapted from Adamson, 1970)

where "0" cooling sequence
"●" heating sequence
"◑" cooling sequence (run 2)
"◐" heating sequence (run 2)

This value is assumed to be equal to γ^{SV} (basal plane of ice-water vapour).

To use equation 3.3.21 to calculate γ^{SV} (basal plane of ice-water) a value of γ^{LV} (liquid-water vapour) must be determined. This was done by using Dorsey's (1968) data for the variation of $d\gamma^{LV}/dT$ with temperature;

$$d\gamma/dT = aT + b \qquad (3.3.24)$$

where T is ^{o}C.

From Dorsey (1968) the value for a is -0.006 dyne/cm - ^{o}C/ ^{o}C and the value for b is -0.139 dyne/cm - ^{o}C.

Integrating equation 3.3.24 between 20^{o}C and -38.8^{o}C yields:

$$\int_{20.}^{-38.8} d\gamma = \int_{20.}^{-38.8} (.0006T + 0.139)\,dT. \qquad (3.3.25)$$

This equation can be further simplified to;

$$\gamma_{-38.8} - \gamma_{20.} = .0003T^2 \Big|_{20.}^{-38.8} - 0.139T \Big|_{20}^{-38.8} \qquad (3.3.26)$$

Using the value of 72.75 dyne/cm (from Dorsey, 1968) at 20^{o}C, the liquid vapour surface tension at -38.8^{o}C is 80.6 dyne/cm. This value agrees with the value obtained from the equation in the A.S.M.E. steam tables (1977).

Substituting the values of γ^{SV} and γ^{LV} into equation 3.3.21 gives a vlue of 17.0 dyne/cm for the basal plane of ice-water interfacial tension. By using equation 3.3.9 from the previous section a value of 28.9 dyne/cm is calculated

for the liquid solid interfacial tension for the prismatic planes. The values of h_1 and h_2 calculated from equations 3.2.3 and 3.2.4 are shown in Figure 3.9.

As shown earlier the values of surface tension for the balas and prismatic planes are insensitive to the chosen value of J, the rate at which the nuclei form. It is also evident that these values will be equally insensitive to changes in Z, the rate constant. A 6% change in the calculated value of γ_1^{SL} will change γ_2^{SL} by 3%. A $1^{\circ}C$ change in the estimated subcooling of $-38.8^{\circ}C$ will change γ_1^{SL} by 1% and γ_2^{SL} by 3%. The values of γ_1^{SL} and γ_2^{SL} are very sensitive to the estimated liquid-vapour surface tension. A change in γ^{LV} of only 5% causes a 36% change in the calculated value of γ_1^{SL} and a 25% change in the calculated value of γ_2^{SL}.

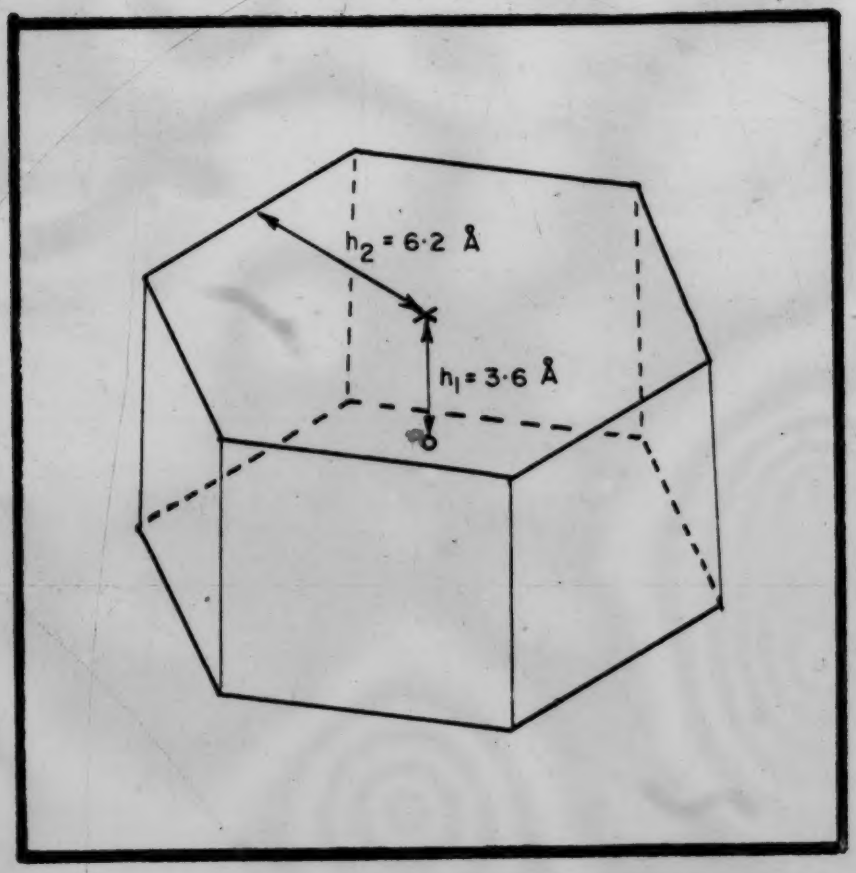

Figure 3.9 Diagram of Proposed Ice Crystal Nucleus
(drawn to relative scale)

4.0 Discussion

Evidence by Simpson et al. (1974a, 1974b) and Hillig (1958) indicates that there is an orientational dependence of the surface tension for ice-water systems. Kallungal (1975) believes that "since ice crystals show definite preferred orientation in growth the γ associated with each of the growth directions should be considerably different."

The values of 17.0 dyne/cm for the basal plane and 28.9 dyne/cm for the prismatic plane (both at -38.8°C) are consistent with what Ketchum and Hobbs (1969) observed. They noted that "when the basal plane was exposed at a grain boundary, the groove was generally asymmetrical, and the results indicated that the surface energy of the basal plane was slightly lower than that of the other crystallographic faces" (Hobbs, 1974). Higuchi (1961) also found that "the basal plane probably has the lowest value of the surface energy of all planes in ice" (Hobbs, 1974). Ketchum and Hobbs (1969) note that only 3% of their total number of datum points include cases where the basal plane was exposed at the grain boundary groove. This means that their value of (29 ± 3) dyne/cm at 0°C which they extrapolate to (25 ± 3) dyne/cm at -40°C is primarily that of the prismatic plane. This value agrees well with the value of 28.9 dyne/cm obtained in this work.

Experiments done by Ketchum and Hobbs (1967) indicate that an ice crystal will tend to grow in a direction

perpendicular to its c-axis in subcooled water. These results are corroborated by experiments conducted by Fernandez (1967 a) Poisot (1968), Vlahakis (1972), Simpson et al. (1974 b) and Huige and Thyseen (1969). Ketchum and Hobbs (1967) propose that a direction parallel to the basal plane is the preferred direction of growth for a crystal because it will maximize the low-energy basal surface. This is consistent with the values obtained in this paper.

A disadvantage of this method is that it yields values of γ_1^{SL} and γ_2^{SL} at only one temperature - that of the homogeneous nucleation point. To compare the values at -38.8°C to those of other researchers at 0°C it is necessary to determine how γ_1^{SL} and γ_2^{SL} vary with respect to temperature ie:

$$\partial \gamma_1^{SL} / \partial T \qquad (4.0.1)$$

and

$$\partial \gamma_2^{SL} / \partial T \qquad (4.0.2)$$

in order to extrapolate the surface energies.

Figure 4.1[1] is a graph of the variation of $\partial \gamma_1^{SL} / \partial T$ with temperature. From this graph it is seen that,

$$\partial \gamma_1^{SL} / \partial T = 0.132 \text{ dyne/cm/}^{\circ}\text{C} \qquad (4.0.3)$$

Isolating γ_2^{SL} from equation 3.2.8 and differentiating with respect to temperature yields

---

[1]The points on the graph are calculated from Adamson's contact angle data at various temperatures, Ward's equations of state and Young's equation.

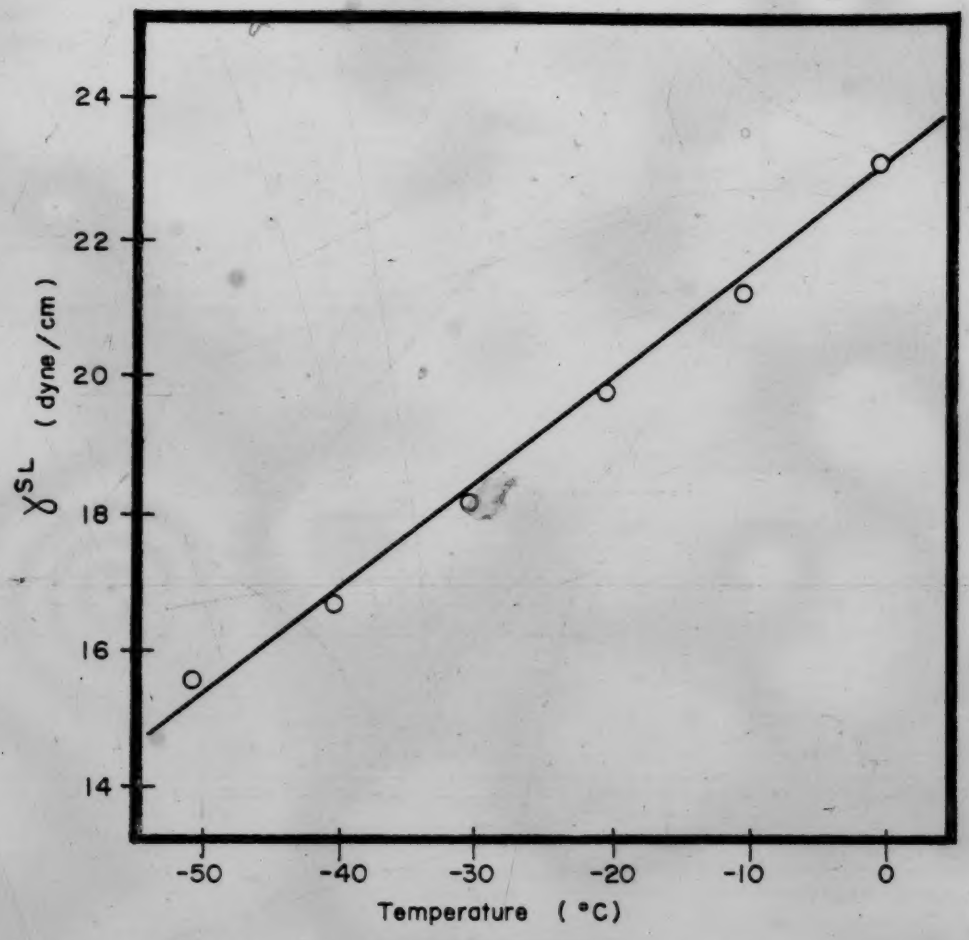

Figure 4.1 Variation of Liquid-Solid Interfacial Surface Tension for the Basal Plane of Ice with Temperature

$$\partial\gamma_2^{SL}/\partial T = Q\left\{\left[\ln(T_0/T)\frac{1}{2\sqrt{T}} - \frac{1}{\sqrt{T}}\right]/\sqrt{\gamma_1^{SL}}\right.$$

$$\left. - \left[\ln(T_0/T)\sqrt{T}\right]1/2\,(\partial\gamma_1^{SL}/\partial T)\sqrt{\gamma_1^{SL}}\right\}, \qquad (4.0.4)$$

where

$$Q = \ln(z)\,K\,\langle L\rangle^2/(48\cot 60^\circ\, v''^2), \qquad (4.4.5)$$

and the temperature dependence of $\ln z$, K, $\langle L\rangle$, and v'' is ignored. At 38.8°C

$$\partial\gamma_2^{SL}/\partial T = -.98 \qquad (4.0.6)$$

Thus at 0°C the values of γ_1^{SL} and γ_2^{SL} are:

$$\gamma_1^{SL} = 22.0 \text{ dyne/cm} \qquad (4.0.7)$$

and

$$\gamma_2^{SL} = 0.0 \text{ dyne/cm} \qquad (4.0.8)$$

(no neg values allowed).

These values for γ_1^{SL}, the solid-liquid surface tension, are not intended to be presented as accurate, because the calculated values for the slopes are valid at -38.8°C but are not necessarily at 0°C. The slope of $\partial\gamma_2^{SL}/\partial T$ is larger than Hobbs' (1974:441) suggested range of 0.1 to 0.35 dyne/cm/°C. It is however interesting to note that $\partial\gamma_1^{SL}/\partial T$ is positive and $\partial\gamma_2^{SL}/\partial T$ is negative. This indicates that the γ_1^{SL} values of γ_1^{SL} and γ_2^{SL} could approach each other as the temperature approaches 0°C. This could explain why most researchers do not notice any orientational dependence for solid-liquid surface tensions at 0°C. It is suggested that the anisotropy of the solid liquid interfacial tension

becomes more prominent as temperature decreases.

Further experimentation is required to verify the results proposed in this paper. In general there is an orientational dependence on surface tension in ice-water systems and the basal plane (as expected) has the lower surface tension.

The approach here is equally applicable to other liquid-solid-vapour systems.

4.1 Conclusions

1. There is anisotropy of γ_1^{SL} in the ice-water-water vapour system at -38.8 °C.
2. Using equilibrium theory, and homogeneous nucleation theory and experimental data, it is possible to generate a relationship between the solid-liquid surface tensions of an assumed nucleus shape.
3. For ice-water this relationship is

$$\gamma_1^{SL}(\gamma_2^{SL})^2 = 1.4 \times 10^4 \ (\text{dyne}^3/\text{cm}^3) \qquad (4.1.1)$$

4. For ice-water at -38.8°C.

$$\gamma_1^{SL} = 17.0 \text{ dyne/cm} \qquad (4.1.2)$$

$$\gamma_2^{SL} = 28.9 \text{ dyne/cm} \qquad (4.1.3)$$

References

Adamson, A.W., J. Colloid, Interfac. Sci. Vol. 34, 1970 pp 461-468.

A.S.M.E. (1977) American Society of Mechanical Engineering, Steam Tables.

Becker, R. (1938) Ann. de Physik, Vol. 32, pp 128.

Callen, H.B. (1960) Thermodynamics. John Wiley and Sons, Inc., New York.

Carte, A.E. (1956) Proc. Phys. Soc., Vol. 69, pp. 1028-1037.

Davies, J.T. and Rideal, E.K. (1963) Interfacial Phenomena. Academic Press, New York.

Defay, R. and Prigogine, I. (1966) Surface Tension and Adsorption. John Wiley and Sons Inc., New York.

Dorsey, N.E. (1966) Properties of Ordinary Water-substance in all its phases: water-vapour, water and all the ices. Hafner, New york.

Dufour, L. and Defay R. (1963) Thermodynamics of Clouds. Academic Press, New York.

Fernandez, R. (1967 a) The Growth of Ice in Flowing Water and NaCl Solutions, Ph.D. Thesis, Syracuse University.

Fernandez, R. and Barduhn, A.J. (1967 b) Desalination Vol. 34, pp 330-342.

Fletcher, N.H. (1959) J. Chem. Phys., (Vol. 31, pp 1476-1482.

Frenkle, J. (1946) Kinetic Theory of Liquids, Oxford University Press. p 488.

Gibbs, J.W. (1961) Scientific Papers of J. Willard Gibbs, Vol. 1, Thermodynamics, Dover Publication p. 325.

Glandorff, P. and Progogine, I. Thermodynamics of Structure, Stability and Fluctuations, (1971) Wiley Interscience, N.Y.

Hardy, S.C., Coriell, S.R. and Sekerka (1971). J. Crystal Growth, Vol. 11, pp. 53-67.

Hellwig, G.E. and Neumann, A.W., (1968) 5th Intern. Congr. Surface Activity, Barcelona Section B, p 687.

Hesstvedt, E. (1964) Norges Geotekniske Institute Publication, Vol. 56, pp 7-10.

Higuchi, K. (1961). On the Shapes of Crystals. J. Met. Soc. Japan, Vol. 39, pp 237-48.

Hillig, W.B. (1958), Growth and Perfection of Crystals. editors R.H. Doremus, et al, Wiley, New York, pp 350-359.

Hobbs, P.V. (1974), Ice Physics, Clarendon Press, Oxford.

Huige, N.J.J., and Thyssen, H.A.C. (1969), Industrial Crystallization, Hodgsen and Son, Ltd., London, pp 69-86.

Jacobi, W. (1955) Z. natuforsch, Vol. 10a, pp 322-330.

Jones, D.R.H. (1970) Ph.D. Thesis, Cambridge University.

Jones, D.R.H. and Chadwick, G.A. (1971). J. Crystal Growth, Vol. 11, pp 260-264.

Jones, D.H.R.. (1973) Phil. Mag., Vol. 27, pp 569-684.

Kallungal, J.P. (1975) Ph.D. Thesis, Syracuse University.

Ketchum, W.M. and Hobbs, P.V. (1967). J. Crystal Growth, Vol. 1, pp 263-270.

Ketchum, W.M. and Hobbs, P.V. (1969). Phil. Mag., Vol. 19, pp 1161-1174.

Kotler, G.R. and Tarshis, L.A. (1968). J. Crystal Growth, Vol. 3, 4, pp 603-610.

Mason, B.J. (1952). Q.Jl.R. Met. Soc., Vol. 78, pp 22-27.

Matijevic, E. (1969). Surface and Colloid Science, Vol. 1.

McDonald, J.E. (1953). J. Met., Vol. 10, pp 416-433.

Poisot, J.M. (1968) M.S. Thesis, Syracuse University.

Pound, G.M., Madonna, L.A., and Plake, S.L. (1953). J. Colloid Sci., Vol. 8, p 187.

Schaefer, V.J. (1948). Bull. Am. Met. Soc., Vol. 29, pp 175-182.

Simpson, H.C., Beggs, G.C. and Deans, J. (1974 a). Private Communication with Allen J. Barduhn.

Simpson, H.C., Beggs, G.C., Deans, J. and Nakamura, J. (1974 b) Desalination, Vol. 14, pp 341-357.

Skapski, A.S. (1956) Acta. Met., Vol. 4, pp 570-582.

Skapski, A.S., Adam, S., Billups, R., and Rooney, A. (1957). J. Chem. Phys., Vol. 26, pp. 1350-1351.

Suzuki, S., and Kuroiwa, D. (1972). J. Calciol., Vol. 11, pp 265-277.

Tucker, A.S., and Ward, C.A. (1975). J. Appl. Phys., Vol. 46, p 4801.

Turnbull, D. and Fisher, J.C. (1949). J. Chem. Phys., Vol. 17, p 71.

Turnbull, D. (1950). J. Appl. Phys., Vol. 21, pp. 1022-1028.

Turnbull, D. (1952). J. Chem. Phys., Vol. 20, pp 411-424.

Turnbull, D. (1965). Liquids: Structure Properties, Solid Interactions, Elsevier Pub. Co., New york, pp 6-24.

Vlahakis, J.G. (1972). Ph.D. Thesis, Syracuse University.

Ward, C.A., and Neumann, A.W. (1974). J. Colloid Interfac. Sci., Vol. 49, No.2.

Ward, C.A. (1975). Private Communication to T. Forest.

Weickman, H. (1949), Ber. Deutsch, Wetterd. U.S. Zone, Vol. 6, p 54.

Whalen, J.W. and Wade, W.H. (1967). J. Colloid and Interfac. Sci., Vol. 24, pp 372.

Whalen, J.W. (1968). J. Colloid Interfac. Sci., Vol. 28, p 443.

Young, T. (1805). Phil. Trans. Roy. Soc. (London), Vol. 95, p 65.

Appendix I: Properties of Water

$L = 333.475 \times 10^{7}$ ergs/g

$v'' = 1.0906$ cm^3/g

$T_o = 273.2^{\circ}K$

$T = 234.4^{\circ}K$

$K = 1.38054 \times 10^{-16}$ $erg/^{\circ}K$

$h = 6.62554 \times 10^{-27}$ erg/s

$n = 3.067075 \times 10^{22}$ molecules

Appendix II: Geometric Relationship of Area in Crystal

Euler's relationship between the area and the linear dimensions is a second order homogeneous function; thus,

$$A^{\beta}(\lambda h_1, \ldots \lambda h_N) = \lambda^2 A^{\beta}(h_1 \ldots h_N) \qquad \text{A.II.1}$$

Differentiating this equation with respect to λ yields

$$\frac{\partial A^{\beta}}{\partial(\lambda h_1)} \cdot \frac{\partial(\lambda h_1)}{\partial \lambda} + \ldots \frac{\partial A^{\beta}}{\partial(\lambda h_N)} \cdot \frac{\partial(\lambda h_N)}{\partial \lambda} = 2\lambda A^{\beta}(h_1 \ldots h_N) \qquad \text{A.II.2}$$

Since this is true for all is set equal to 1. Rearranging the terms yields:

$$A^{\beta} = \tfrac{1}{2} \sum_{\alpha} h^{\alpha} \frac{dA^{\alpha}}{dh_{\beta}} \qquad \text{A.II.3}$$